FUNCTIONALIZED SINGLE-WALLED CARBON NANOTUBE CHEMIRESISTIVE SENSORS FOR VAPOR DETECTION OF EXPLOSIVES AND DRUGS

by

Yaqiong Zhang

A dissertation submitted to the faculty of
The University of Utah
in partial fulfillment of the requirements for the degree of

Doctor of Philosophy

Department of Materials Science and Engineering

The University of Utah

December 2017

The University of Utah Graduate School

STATEMENT OF DISSERTATION APPROVAL

The dissertation of **Yaqiong Zhang**

has been approved by the following supervisory committee members:

Ling Zang	, Chair	**08/11/2017** Date Approved
Michael A. Scarpulla	, Member	**08/11/2017** Date Approved
Hanseup Kim	, Member	**08/11/2017** Date Approved
Jordan Gerton	, Member	**08/11/2017** Date Approved
Shelley D. Minteer	, Member	**08/11/2017** Date Approved

and by **Feng Liu** , Chair of the Department of **Materials Science and Engineering**

and by David B. Kieda, Dean of The Graduate School.

ABSTRACT

Explosives and drugs cause problems in society when used inappropriately. It is highly desired to detect these chemicals in a quick and reliable way with low cost. Vapor detection of explosives and drugs has been proven to be one of the most effective, practical, and noninvasive methods. Among all the methods developed so far, highly sensitive carbon nanotube-based (CNT-based) chemiresistive sensors remain promising. In this dissertation, we explored and developed three CNT-based sensors for the explosive and drug detection.

In this dissertation, we proposed that the dominant mechanism of our oligomer-coated CNT-based sensors is due to the swelling of the oligomers. Based on this swelling mechanism, we have designed three oligomers or polymers functionalized CNT-based sensors for the detection of nitro-explosives, alkanes (related with ammonium nitrate/fuel oil), and amines (related with methamphetamine), respectively.

Beyond the high sensitivity to the target analytes, the selectivity of the sensors was largely enhanced by the careful selection of oligomers and polymers. The three oligomers and polymers under investigation can enhance the interaction between the sensor and the analyte, and facilitate the dispersion of CNTs in a solution. For the detection of nitro-explosives, we chose an oligomer that had been successfully demonstrated as a fluorescence-based nitro-explosive sensing materials. For the detection of alkanes and amines, we introduced the alkane side chains and carboxylic acid functional groups in the polymer.

This dissertation demonstrated three examples of oligomer or polymer functionalization CNT-based sensors for the detection of explosives and drugs. Meanwhile, the dominant mechanism of the sensors was proposed. This research paved ways for developing chemical vapor sensors with better sensitivity and selectivity in the future.

To my family and friends

TABLE OF CONTENTS

LIST OF FIGURES

Figures

LIST OF ABBREVIATIONS

°C	degree Celsius
µL	microliter
µm	micrometer
3D	three–dimensional
a.u.	arbitrary units
AFM	atomic force microscopy
APhS	trimethoxyphenylsilane
cm	centimeter
CNT	carbon nanotube
CVD	chemical vapor deposition
DMF	dimethylformamide
DMMP	dimethyl methylphosphonate
DNT	dinitrotoluene
ELC	electrochemiluminescence
eq	equivalents
et al.	and others
etc.	and the rest
EtOH	ethanol
FET	field-effect transistor
FTIR	Fourier-transform infrared spectroscopy
GC	gas chromatography
GC-MS	gas chromatography–mass spectrometry
HiPCO	High-pressure carbon monoxide method
IDE	Interdigitated electrode

IMS	ion mobility spectroscopy
L	liter
LDA	linear discriminant analysis
LOD	limit of detection
MEMS	micro-electro-mechanical system
M	$mol \cdot L^{-1}$
mg	milligram
min	minutes
MO	molecular orbitals
MOF	metal-organic framework
MS	mass spectrometry
NA	nitroaromatic
NH_3	ammonia
ng	nanogram
nm	nanometer
NMPA	n-methampethamine
NMPEA	n-methylphenethylamine
NO_2	nitrogen dioxide
NT	nitrotoluene
ODCB	1,2-dichlorobenzene
OSHA	the Occupational Safety and Health Administration
OVA	ovalbumin
P3AT	poly(3-alkylthiophene-2,5-diyl)
P3BT	poly(3-butylthiophene-2,5-diyl)
P3CT	poly(3-(6-carboxyhexyl) thiophene-2,5-diyl))
P3DT	poly(3-dodecylthiophene-2,5-diyl)
P3HT	Poly(3-hexylthiophene-2,5-diyl)
P3OT	poly(3-octylthiophene-2,5-diyl)
Pbi-chol	perylene bisamide derivatives substituted with cholesteryl

PC	photonic crystal
PCA	principle component analysis
PEI	polyethyleneimine
PET	photoinduced electron transfer
PETN	pentaerythritol tetranitrate
PLE	photoluminescence excitation
PMA	1-pyrenemethylamine
ppb	parts per billion
ppm	parts per million
ppq	parts per quadrillion
PTCDI	perylene bisamide derivatives substituted with cholesteryl
RBM	radial breathing mode
RDX	1,3,5-Trinitroperhydro-1,3,5-triazine, wildly used as an explosive
s	second
SAW	surface acoustic wave
sccm	standard cubic centimeter per minute
ssDNA	single-stranded DNA
SWCNT	single-walled carbon nanotube
Tg	triethylene glycol monomethyl ether
Tg-Car	an arbazolylethynylene oligomer
TNP	2,4,6-trinitrophenyl
TNT	trinitrotoluene
UV	ultra-violet
UV-vis	ultra-violet-visible radiation
UV-vis-NIR	ultra-violet-visible-near-infared radiation
π	pi; bond or orbital

ACKNOWLEDGEMENTS

I want to thank my advisor Ling Zang for his consistent and pointed guidance on my research and my dissertation. In retrospect, it was surprising how helpful and precious his advice was. Meanwhile, I greatly appreciate his kindness for giving me the freedom to explore and learn at my own pace. And I appreciate his detailed suggestions on my many presentations and writings. I'm also grateful for his support for my study and research in his lab for over five years.

I would like to thank my committee members, Mike Scarpulla, Hanseup Kim, Shelley Minteer, and Jordan Gerton for their occasional but meaningful guidance and encouragements on my dissertation. I want to thank Hanseup Kim for his time and advice on my career and life. I want to thank Mike Scarpulla for his kindness for sharing lab instruments and tools with me.

I would like to thank my collaborators and colleageus: Xiaomei Yang, Yanke Che, Ligui Li, Jimin Han, Helin Huang, Miao Xu, Benjamin R. Bunes, Daniel L. Jacobs, Chen Wang and Na Wu, Frank Bennion Redd, and also the visiting professors, Aixia Han and Li Yu. I appreciate their help on my study, research, and my life. I miss spending time with them and working on research problems.

I would like to thank my dear friends whom I met in Salt Lake City for the time we spent together and for the fun things we did together. To list a few: Yuying Zhang, Jingzhu Li, Tiantian Liu, Weibka Gerlach, Rui Yan, Qingbo Guo, Xiaowen Wan, Weier Rong,

Lizeth Napan, Pingchuan Ma, and Feifan Zhou.

I would like to thank my son Austin, for making me feel proud and making me laugh. I would like to thank my husband Bing for his love. I would like to thank all the members of my family for their support and confidence.

I am also grateful for the funding support from the Department of Homeland Security, the National Science Foundation and the Utah Science Technology and Research Initiative.

CHAPTER 1

INTRODUCTION

Due to the increased number of terrorism incidents in recent decades (Figure 1.1), explosives (particularly homemade) are considered one of the major threats to society, as well as one of the key problems in the 21st century. Between the years 2011 and 2015, there were 57,201 terrorism incidents worldwide and more than half of the incidents used explosives as a weapon (Figure 1.2) (1). Hidden explosives not only pose a threat to lives in war zones, but also to the public safety worldwide. Some recent terrorist attacks involving explosives include the 2005 London underground bombings (2), the 2013 Boston Marathon bombings (3), and the 2016 Brussels bombings (4). Thus, rapid detection of those hidden explosives, especially in vapor phase, is critical for defending lives against potential terrorist attacks.

While the negative effects of terrorism attacks are often obvious and immediate, illicit drug use gives long-term negative consequences to both drug abusers and their family (5). These negative social consequences of drug abuse include drug-related crimes, disease transmission, child abuse, and environmental damage. Meanwhile, drug use and abuse may lead to prolonged hospital stays and a great loss of productivity. However, the amount of drug usage is large and continues to increase. According to the results from the 2015 National Survey on Drug Use and Health (6), 1 in 10 individuals 12 years or older in the

United States have used illicit drugs in the past month from the time of the survey. Among them, 18.9% were under 18 years old. Thereby, a drug sensor is desired for preventing first time use of those drugs, preventing drug transportation, as well as helping detect clandestine drugs synthesis in places like homes and vehicles.

This dissertation includes the detection of nitro-explosives (such as trinitrotoluene and dinitrotoluene) and improvised explosives made of ammonium nitrate-fuel oil mixture. For the illicit drug detection, this dissertation focuses on the powerful and wide-spread drug, methamphetamine.

The introduction of the dissertation covers several instrumental methods and some emerging techniques for vapor detections of explosives and drugs. The instrumental methods include Ion Mobility Spectrometry (IMS) (7), Gas Chromatography/Mass Spectrometry (GC/MS) (8), and Fourier Transform Infrared Spectroscopy (FTIR) (9). They are usually accurate and precise. However, these instruments are often bulky and expensive, and require specific trainings for operations and maintenance. Emerging techniques, on the other hand, are usually cost effective, small in size, and easy to operate. However, most of these methods are still facing challenges in commercialization and dealing with the complex real-world environment.

1.1 Instrumental Methods for Vapor Detections of Explosives and Drugs

This section of the dissertation introduces several instrumental methods commonly used in vapor detections of explosives and drugs, and focuses on the progress of their minimization and commercialization.

1.1.1 Gas Chromatography/Mass Spectrometry

Gas Chromatography/Mass Spectrometry (GC/MS) is considered the "gold standard" for chemical detections and identifications (10) since there are rarely two chemicals showing identical behavior in both GC and MS. There are two parts in GC/MS, the gas chromatograph and the mass spectrometer (11). The GC part utilizes a capillary column to separate different components in a mixture due to the different mobility of each component. MS is another analytical instrument connected to the GC, which further separates and identifies chemicals. MS works through ionizing the molecules and identifying the molecules by their mass to charge ratios. The combination of GC and MS greatly enhances the capability of the detection.

GUARDION from Smith detection is one of the most portable and commercially available versions of GC/MS in the world. The weight of the whole instrument is 14.6 kg, significantly lighter than the normal bench-top GC/MS instruments. But it is still too heavy for certain situations. The time for each single analysis of GUARDION is about 3 min, while the test from normal GC/MS usually takes hours to complete. The disadvantage of a miniaturization is that it may compromise some of the high performance of GC/MS, like sensitivity.

1.1.2 Ion Mobility Spectrometry

Ion Mobility Spectrometry (IMS) has been widely used for detections of explosives and drugs for military or security purposes (12-15). There are more than 10,000 IMS instruments worldwide in airports and more than 50,000 IMS instruments in the U.S. Army (15). Their popularity is mainly due to their high portability along with their high sensitivity, fast response, low-power consumption, and simplicity of operation. For example, the

commercially available and portable IMS not only has high sensitivity, but can also run each test in a few seconds with four AA batteries.

In IMS, vapor phased samples are ionized and their mobility spectra in a drift tube can be measured (16). Then, the mobility spectra of the samples are compared with the known mobility spectra of threat compounds. If they match, the alarm condition will be triggered in the IMS device. The disadvantages of IMS devices are the high false positive ratio from the complex spectra of some widespread ionizations, and the difficulties of detecting some low ionization potential chemicals. Meanwhile, depletion of some low vapor pressure chemicals (such as RDX and PETN) occurs rapidly and it will be very difficult to reproduce some of the testing results (17).

1.1.3 Fourier-Transform Infrared Spectroscopy

Fourier-Transform Infrared Spectroscopy (FTIR) is another method for vapor detections of explosives and drugs. FTIR measures the infrared light absorption of the sample. It measures each wavelength simultaneously and uses the Fourier transform algorithm to process the sensing data (18). FTIR is commonly used for the identification of chemicals in solid and liquid phases (9). But now, it is also used for field detections of vapors. Some portable FTIR gas and vapor detector systems have a database storing the absorption fingerprints of target chemicals, such as nerve agents, toxic industrial chemicals, and explosives. Once the sample chemical is measured, the absorption fingerprints will be compared with the fingerprints in the database to see if the sample's fingerprints match any of them. In the portable system, there is usually a sample collection device which collect and preconcentrates low concentration samples.

1.2 Emerging Vapor Sensing Methods for the Detection of Explosives and Drugs

1.2.1 Fluorometric Sensors

Fluorometric sensors are based on the fluorescence quenching or fluorescence enhancement of the sensing materials (19-22). The mechanism usually involves the matching of the molecular orbitals (MO) between the sensing materials and the analytes, which makes the photo-induced electron transfer (PET) possible. In addition, the sensing signals can be amplified from the fact that the excitons diffuse along conjugated sensing nanomaterials (23).

Organic molecules or polymers have interesting optical properties that are suitable for the purpose of vapor detection, and they have a wide variety of options for molecular structure and functional group modifications for enhancing their selectivity. Thus, they are good candidates for fluorometric sensors. Conjugated polymers were demonstrated as sensing materials for nitro-related explosives in 1995 in Timothy M. Swager's group (24). The fluorescence of the sensing materials will be quenched by the electro-withdrawing nitro-explosives, and thus the nitro-explosives can be detected (25). The amplification mechanism in the conjugated polymer is based on an energy migration scheme, in which excitons diffuse along the conjugated polymer chain. When one analyte molecule sticks on one site of the polymer chain, the whole conjugation polymer chain will be quenched. For example, poly(phenylene ethynylene) and its related structures were synthesized and tested for the explosive sensing (26-27). Those polymers are usually made as a thin film on a substrate with an optimized thickness. Related molecular structures with different sterically demanding moieties (such as pentiptycene groups) (28) were demonstrated to enhance the diffusion of vapors into the porous thin film, and then improve the sensitivity of the sensor.

A commercialized trace explosive detector named Fido (29) was developed based on the conjugated fluorescent polymers. The detector is ultra-lightweight (less than 1.5 lb), fast (detect in several seconds), and super sensitive to a broad range of explosives.

Another example of conjugated polymers used in sensing nitro-related explosives are those Si-containing polymers and metallole-containing polymers (30-33). In 2011, one of the conjugated polymers were combined photonic crystals (PC) as a TNT vapor sensor (34). The enhancement of fluorescence quenching was achieved by the photonic effect and the large surface area of the PC with an inverse opal structure.

Besides conjugated polymers, there are many other materials (35-36) that can be used as fluorometric sensors. The organic nanofibril based on self-assembled alkoxycarbonyl-substituted carbazole-cornered tetracycle was developed as the sensing materials for vapor of detections of TNT in 2007 (38). Another organic nanofibril based on self-assembled linear carbozole trimers was developed as sensing materials for vapor detections of TNT in 2010 (39). Metal-organic frameworks (MOF) were reported as the sensing materials in a nitro-explosive sensor in 2013, using triphenylene-2,6,10-tricarboxylate and Tb^{3+} as the building blocks (37). The MOFs were stable up to 500 °C and have shown selective sensing for different nitroaromatic explosives.

Sensors for amine-related drugs, such as n-methamphetamine (NMPA) and ketamine, have often been seen as fluorescence enhancement sensors due to the electro-donating properties of the amine-related drugs. This fluorescence enhancement phenomenon was demonstrated in a copolymer sensor based on benzothiadiazole (40), and a polymer thin film sensor based on perylene bisamide derivatives substituted with cholesteryl moiety (PBI-Chol) (41).

1.2.2 Colorimetric Sensors

Colorimetric sensors are based on the absorption changes of the sensing materials in the visible range. Compared with fluorescence sensors, colorimetric sensors do not require excitation light. The pH test strip is a good example of a colorimetric sensor, which is very simple and convenient to use. Researchers have developed a lot of colorimetric sensors, and their mechanisms range from aggregation induced color change of sensing materials to chemical reactions between the sensing materials and the analyte (42-44). However, most of the colorimetric sensors reported are testing liquid samples (45-48). There are only a few reports that are testing vapor samples and usually require optical enhancement component like waveguide micro-ring resonators or fiber Bragg structures to amplify the sensing signal.

1.2.3 Chemiresistive Sensors

Chemiresistive sensors are good for applications that require high portability, large covering area, and contineouse testing due to their simplicity. The candidate materials for making a chemiresisitve sensor include: metal-oxide nanomaterials (49-51), carbon black\polymer (52), self-assembled PTCDI nanowires (53-54), and other semiconductor materials (55-57).

The technology of metal-oxide chemical sensors is matured and has been successfully commercialized. It was first studied in 1962 in Japan with zinc oxide thin films (58). After that study, many new metal-oxides and doped metal-oxides have been studied and developed as sensing materials. The morphologies of the materials vary from 0-dimensional nano-particles to two-dimensional (2D) thin films. The sensing mechanism is highly depended on the surface interaction between the sensing materials and the analytes.

The O^- on the sensor's surface is believed to play a vital role in the whole sensing process, which has the best working temperature at 300 °C to 450 °C. The performances of the sensors are affected by their microstructures, materials components, surface-modification as well as their operational temperatures. In 2012, an "electronic nose" was developed for the detection of explosives (TNT, PETN, and RDX) using 12 commercially available metal-oxide sensors (51).

Chemiresistive sensors based on carbon-black/polymers have been extensively studied in the 1990s in N. S. Lewis' group from California Institute of Technology. These chemiresistive sensors are based on the swelling of the polymer matrix when exposed to the analytes; and the swelling of the polymer matrix will loosen the conducting network of carbon black, and decrease conductivity (52). A sensor array made of carbon-black with different polymers was evaluated as an "electronic nose" for distinguishing different analytes in Lewis' group.

Another kind of chemiresistive sensors are the sensors based on organic one-dementional (1D) materials with enhanced conductivity through the intra-molecular charge transfer in the materials. The charge transfer was enabled by the electron donor-accept (D-A) systems in the molecules of the nanofiber. In 2010, nanoribbons made of perylene tetracarboxylic diimide (PTCDI) backbones with different side chains were used for the detection of nitro-explosives (54). The sensor showed sensitive responses to the vapors of nitromethane and other nitro-explosives, whereas there was no significant response towards the vapors of aniline, ethanol, acetone, and acetonitrile. Vaporsens (59), a University of Utah spinoff in Salt Lake City was founded in 2011 and has been working on these vapor sensors.

Other sensing materials include gold nanoparticles (57), carbon nanotubes (which will

be discussed in detail later), 2D materials such as graphene (60) and MoS_2 (61). They all share the same advantages such as simple operations and low costs.

1.2.4 Others

Other sensors that have been commercialized or have shown great potential for commercialization include sensors based on capacity measurements (62), micro-electro-mechanical system (MEMS) (62-63), surface acoustic wave (SAW) measurements (64), and the electrochemical sensors (22). There are two types of those sensors, one is the sensor designed with no surface modifications, the other one is the sensor designed with surface modifications. Sensors designed with no surface modifications rely on the physical properties of analytes for their sensing purpose. For example, a MEMS sensor array (65) for the detection of explosive particles works by heating the silicon beam to the melting temperature of a target analyte, and the heat absorption of the analyte was measured at that temperature. This sensor can detect TNT and RDX samples down to 1 μg. Sensors with surface modifications have a layer of molecules that can enhance the interaction between the sensor and the analyte. For example, sensor platforms based on AFM cantilevers coated with a layer of APhS (trimethoxyphenylsilane) molecules were developed, which were able to detect TNT vapors as low as at part-per-trillion (ppt) levels. (62). The APhS layer facilitates the surface absorption of TNT on that surface.

1.3 Motivations of CNT-based Sensors for Vapor Detections of Explosives and Drugs

Although there are many vapor sensors commercially available and have shown successful applications in many area, every sensor has its drawbacks at some point. For

example, the fluorescence-based sensors suffer from complex and space-demanding optical components which illuminate the sensor. Chemical reaction-based colorimetric sensors usually show limited sensitivity to vapors. This is probably due to the fact that most of the chemical reactions happen only in solutions, or only in high concentrations of vapors.

Chemiresitive sensors based on CNTs, graphene (67-68), and MoS_2 (69) are attractive candidates since they do not require illuminations and have shown great sensitivities to vapors. Among them, CNTs have several advantages superior to the 2D materials (such as graphene and MoS_2) (70). First, the conductivity of a CNT can be completely "turned-off" by an absorbed molecule on one site the surface, since the penetration depth of the absorbed molecule's influence on the electrical property of the CNT may exceed the entire diameter of the CNT. However, for 2D materials, this direct "turn-off" is difficult to realize with one attached molecule. Second, the bandgaps of CNT can be selected by the choice of their diameters. In comparison, some 2D materials, such as graphene, are zero bandgap semiconductors, meaning that the conductivity of these materials is difficult to switch off.

CNT-based chemiresisitve sensors have other unique advantages: first of all, the surface of CNTs can be chemically functionalized to afford specific bindings with certain analytes. CNTs are like the "playground" for all kinds of nano-sized reactions and interactions. Second, after so many years of intense study of CNTs, the growth and purification methods are well developed. Third, new techniques of CNT dispersion and manipulation, such as CNT ink and CNT alignment, was discovered. With all those advantages of CNTs, it is highly promising to make a new generation of low-cost, portable, and highly sensitive and selective vapor sensors.

1.4 Basics of Carbon Nanotubes

Carbon nanotubes have been officially discovered by Sumio Iijima in 1991 (71). That paper about this discovery has been cited over 40,000 times. In that paper, the structure of a multiwalled CNT was characterized using a high-resolution transmission electron microscopy (HRTEM). In 1993, the first single-walled carbon nanotubes (SWCNT) (72) was discovered by the same research group. Before Iijima's discovery, there were reports about observing tubular structures of carbon via electron microscopy, as well as theoretical calculations predicting the properties of CNTs. However, these earlier works did not attract the broad attention as today at that time. With the rapid development of nanotechnologies (73), CNTs have attracted much more attention in the past decades, largely driven by their unique properties and great potential for applications in optoelectronics devices, including chemical sensors.

1.4.1 Structure and Electrical Properties

CNTs represent the 1D nanomaterials in the family of fullerene (graphene as the 2D nanomaterials and bukyminsterfullorene/C_{60} as the zero-dimentional nanomaterials). A single-walled carbon nanotube can be seen as rolling a layer of graphene into a tube. The geometry of a CNT can be fully represented by the direction of rolling represented in terms of a chiral vector *C (C = na_1 + ma_2)*, *a1*, *a2* are unit vectors of graphene. We can use the two integers *n* and *m* to fully represent the geometry of the CNT. The diameter of a CNT can be calculated with the equation shown below (74):

$$d = \frac{a_{cc}\sqrt{3(m^2 + mn + n^2)}}{\pi} = \frac{C}{\pi} \tag{1.1}$$

where a_{cc} is the carbon-to-carbon bond length, *C* is the length of the chiral vector.

The chiral angle θ is defined as the angle between C and a_1. (Figure 1.3) There are two special structures, one is the zigzag (m=0), the other is the armchair (n=m). The electric properties of CNTs are significantly related with m and n. When $|n-m| = 3q$ (q is an integer), the nanotube is metallic or semimetallic. Otherwise, the nanotube is semiconducting. CNTs also exists as single-walled CNTs and multiwalled CNTs.

1.4.2 Carbon Nanotube Growth Methods

The performances of CNT-based sensors depend on the structure and the quality (purity, amount of metal catalyst residuals, and the amounts of defects) of the CNTs used in that study, which are affected by their growth methods. Although postsynthesis processes help improve the quality of CNTs, a good fabrication method will save a lot of time and effort for achieving good quality CNTs.

Commonly seen growth methods are Arc Discharge (76-77), Laser Ablation (78-79), and Gas Phase Process (80-81). Arc Discharge and Laser Ablation methods produce the highest quality of CNTs in terms of the number of defects. However, these methods either involve an electrical discharge from carbon-based electrodes or involve expensive high-energy lasers to interact with the graphite source, and their yields are low and their impurity amounts are high. Gas Phase Process, also known as the Chemical Vapor Deposition method is a popular method. It utilizes a hot furnace, a carbon source in gas phase (such as, CO, methane, and benzene), and substrates with metal catalysts. The yield is high with fewer impurities in the product, thus, it's suitable for large-scale productions of CNTs. The high-pressure carbon monoxide method (HiPCO) developed in Rice University was one of the most widely used method for the synthesis of high purity, and small-diameter SWCNT and has shown great commercial success.

1.4.3 Dispersion Enhancement Methods

CNT dispersion means de-bundle and stabilize CNTs in a solution, while CNTs usually cluster together and precipitate in most solutions. In addition, some dispersion methods can selectively disperse CNTs with certain chiralities, and can separate impurities from the growing process of CNTs. The majority of CNT dispersion methods that have been developed, rely on functionalizations of CNTs. Those methods can be classified into two categories, one is covalent functionalization-related methods and the other is noncovalent functionalization-related method. Noncovalent functionalization-related methods will not disturb the structure of the nanotube, and will not cause changes in the electrical properties of CNTs. These methods were usually developed by using surfactant (82-83) (such as sodium dodecyl sulfate), conjugated oligomers (84), conjugated polymers (85-86) (P3HT derivatives), small molecules (87) (azobenzene derivative), and single-stranded DNA (ssDNA) (88).

The dispersion of CNTs can be characterized by their absorption spectra, photoluminescence excitation (PLE) spectroscopy, and Raman spectroscopy. Absorption spectra and PLE are used to identify the species of CNTs. The Raman spectroscopy is used for identifying the defects of CNTs, and the radial breathing mode (RBM) of a Raman spectroscopy can be used for indicating the surface interaction between the functionalization molecule and the CNT (89). For example, an up-shift in the RBM was observed for the oligomer (mPE-13mer) functionalized CNTs compared with the as-received CNTs in the study reported by Zang's group (84).

Noncovalent functionalization-related methods were usually using molecules that have one part of them (such as the backbone of the polymer and the nucleobase of the DNA) strongly react (pi-pi stacking or van der Waals interaction) with CNTs, and having another

part of the molecule (such as the functional group in DNA or the sided chain in a polymer) strongly react with the solution, which is similar with the commonly known mechanism of a surfactant (90). Subtle changes of the dispersion molecules, such as weight, backbone rigidity, the side chains (74, 85, 91-92), and changes of the dispersion environment (85) can often lead to dramatic differences in the dispersion results.

1.5 Carbon Nanotube Sensors for Vapor Detections of Explosives and Drugs

1.5.1 Intrinsic Carbon Nanotube Sensors

In 2000, two similar reports (94-95) in the same volume of *Science* magazine demonstrated for the first time, that an as-grown CNT can be used in chemical sensors. They observed that the conductance of a single-walled carbon nanotube (SWCNT) increased when exposed to NO_2 (2 to 200 ppm) and decreased when exposed to NH_3 (0.1 to 1%). Although there are still debates on the mechanisms of the intrinsic sensors, the mechanisms were usually explained by the charge transfer between the analyte and the p-type SWCNT (96). In the charge transfer mechanism, NO_2 has an unpaired electron and is known an electron-withdrawer and NH_3 has a long electron pair and is known as an electron-donator. In order to control the alignment of CNTs in the device, a SWCNT sensor (97) was fabricated from transferring a SWCNT "forest" grown with chemical vapor deposition (CVD) to a fabric substrate. The sensor with aligned CNTs showed a detection limit of 8 ppb to TNT molecules and 40 ppb to NO_2 molecules.

One challenge of intrinsic CNT sensors is that their conductivities are usually difficult to recover after the exposure to analytes. In the report from Kong and her coauthors (94), the sensor was able to recover under the ambient condition or by heating at high

temperatures. Another report in 2001 (98) found that upon ultraviolet (UV) illumination, the conductivity of a SWCNT sensor quickly recovered to the conductance level before the exposure. They suggested that this desorption process is not due to a thermal process, but due to the photo excited plasmon in SWCNTs. In 2012, an intrinsic sensor was reported (99) by using in situ UV light illuminations to enhance the performance of the sensor by orders of magnitude. The detection limit obtained for NO_2 was 590 ppq (parts-per-quadrillion).

1.5.2 Covalently Functionalized Carbon Nanotube Sensors

Covalent functionalizations happen at the end of the nanotube, defect sites of the nanotube, as well as the side-wall of the nanotube. Early research on covalent functionalization of CNTs has benefited from the relatively well-developed covalent surface chemistry of fullerenes at that time. These functionalization methods include fluorination, ozonolysis, organic functionalization, and osmylation (100-101). Raman and FTIR spectroscopy can be used for verifying covalent functionalizations and identifying the functional groups introduced in the functionalizations (102-103).

In 2010, a sensor array (104) was made of convalently functionalized CNTs to selectively detect common VOCs. The selective recognition groups were covalently added into the CNT via zwitterionic and post-transformation synthesis procedures. The selectors were able to increase the interaction between the CNTs and the analytes through hydrogen bondings, induction intermolecular forces (also known as polarization), and dispersion intermolecular forces (also known as London force). In 2012, another sensor array (105) was made of CNTs covalently functionalized with functional groups containing selector unites for the detection of cyclohexanone and nitromethane explosives. The sensor array

showed sensitivity to part-per-million (ppm) levels of those explosive analytes and showed a clear response to the analytes after standing in ambient for 8 months after fabrication. The good stability of covalent functionalized CNT sensors is an advantage comparing with noncovalently functionalized CNT sensors.

1.5.3 Noncovalently Functionalized Carbon Nanotube Sensors

Noncovalent functionalizations use a wide variety of materials, including biomolecules (such as DNA (106-107), peptides (108), antibodies (109)), polymers (110-116), oligomers (117), organic small molecules (118-120), self-assembled monolayers of organic molecules (121), inorganic nonmetal nanoparticles (122), as well as metal nanoparticles (114).

Biomolecules often provide a specific binding site for an analyte. For example, in 2010, a CNT-based immune-sensor (109) was developed for the detection of TNT in water. 2,4,6-trinitrophenyl (TNP) coupled ovalbumin (OVA), and anti-TNP single chain antibody (scab) was used in this study. One year later, Strano's group developed a TNT sensor (108) based on the conformation of the near-infrared fluorescence of an individual CNT. In their study, a class of peptides from the bombolitin family were used for the nitroaromatic recognition. They claimed that single molecule recognition of TNT using the amphipathic bombolitin II oligopeptide modified CNT. In the same year, CNT-based field-effect transistor (FET) was developed using a TNT receptor and the conjugated polydiacetylene. The sensor was able to selectively detect TNT at 1 fM in real-time. All those biomolecule-modified CNT sensors have good selectivities. However, all those sensors can only be used for samples in water solutions due to the limitation of using biomolecules.

Polymers/CNT sensors are more commonly seen since there are many conjugated polymers have been found to facilitate the dispersion of CNT in solutions and a vast variety of polymers with different backbones and functional groups that can be selected. Early in 2003, Dai's group applied two polymers to enhance the selectivity of CNT sensors (110). One of the polymers used for coating CNT thin film is polyethyleneimine, which makes the sensor n-type and can selectively respond to NO_2, while will not response to NH_3. The other polymer is polymeric perfluorinated sulfonic acid ionomer (Nafion) which makes the sensor selectively response to NH_3 and blocks NO_2. In 2005, Snow's group (121) were the first to establish a SWCNT capacitor sensor with a thin film of hexafluoroacetone covered CNTs for the detection of trace DMMP ranging from 320 ppb to 2.9 ppm. In 2011, Star's group investigated the mechanism of a polyaniline-coated CNT chemical sensor (113) towards the detection of NH_3, acetic acid, and hydrazine. The sensor showed recoverable responses towards hydrazine. The electron-doping mechanism was demonstrated by electrochemical measurements and UV-vis-NIR spectra. In the same year, Lu and coauthors developed a sensor (114) based on polyethyleneimine (PEI) functionalized SWCNTs capable of sensing H_2O_2 at 25 ppm.

There are many examples of functionalized CNT sensors in the field of explosive and drug detecting. For example, sensors which are based on 1-pyrenemethylamine (PMA) functionalized CNTs were reported for the testing of the TNT in water (120). The amine functional group in PMA was supposed to electively bind with TNT and form a negative charged complex on the surface of CNTs. The sensor showed obvious responses to TNT at the concentration of 1 ppt. Lu and coauthors reported a sensor based on CNTs functionalized with porphyrin for the detection of 3-dinitrobenzene vapor (118).

1.5.4 Carbon Nanotube Sensor Arrays

Olfactory sensation is one of the five senses through which we perceive the world around us. It is estimated that humans can sense as many as 10,000 to 100,000 chemicals as distinct odors (123). Linda Brown Buck and Richard Axel's work on understanding how the olfactory sensation works won the 2004 Nobel Prize in Medicine. We can see a sensor array coupled with a computer with artificial intelligence as an olfactory system. However, the olfactory system, which has been optimized by the evolution, is a much mature and sophisticated one. We may want to learn from it for the future development of sensor array systems.

Electrical sensors based on chemiresistive or FET could easily be adapted and combined into a sensor array system (124-125). Actually, the sensor array topic has been extensively studied in Lewis's research group using carbon black/polymer sensors (126). Principle component analysis (PCA) analysis (52), (127-128) were reported for distinguishing the types and concentrations of analytes. Later on, CNT-based sensors become a popular material for making chemical sensor arrays. And more sophisticated data analysis (129) and machine learning techniques (130) have brought into the visualizations and predictions of sensor array systems, and would be the future trend.

1.6 Objectives of this Dissertation

When judging the performance of a chemical sensor, we look at its sensitivity, limit of detection (LOD), selectivity, reversibility, resolution (smallest concentration variation which can be detected), dynamic range (the concentration between LOD and the maximum detectable concentration), and response time. The emphasis of this dissertation is enhancing the selectivity of CNT-based vapor sensors in order to enhance the performance

of it.

The objectives of this dissertation are:

1. Develop fabrication methods for the noncovalently functionalized CNT-based sensors.

2. Explore the mechanism of the oligomer-coated CNT sensor, and develop a sensor for the selective detection of nitro-explosives.

3. Explore the effect of alkyl side chain lengths on the selective sensing of different sizes of linear alkanes vapors, and develop a sensor for the selective detection of alkanes.

4. Explore the effect of carboxyl functional groups on the selective sensing of amines, and develop an amine-related drug (e.g., methamphetamine) sensor.

1.7 References

(1) National Consortium for the Study of Terrorism and Responses to Terrorism, Global Terrorism Database, https://www.start.umd.edu/gtd/ (accessed October 20, 2017).

(2) McKenna, B.; Waddell, N. Media-ted Political Oratory Following Terrorist Events: International Political Responses to the 2005 London Bombing. *J. Lang. Polit.* **2007**, *6,* 377-399.

(3) Gates, J. D.; Arabian, S.; Biddinger, P.; Blansfield, J.; Burke, P.; Chung, S.; Fischer, J.; Friedman, F.; Gervasini, A.; Goralnick, E.; Gupta, A.; Larentzakis, A.; McMahon, M.; Mella, J.; Michaud, Y.; Mooney, D.; Rabinovici, R.; Sweet, D.; Ulrich, A.; Velmahos, G.; Weber, C.; Yaffe, M. B. The Initial Response to the Boston Marathon Bombing: Lessons Learned to Prepare for the Next Disaster. *Ann. Surg.* **2014**, *260,* 960-966.

(4) Kolaric, S.; Schiereck, D. Are Stock Markets Efficient in the Face of Fear? Evidence from the Terrorist Attacks in Paris and Brussels. *Finance Res. Lett.* **2016**, *18,* 306-310.

(5) Ostler, T.; Bahar, O. S.; Jessee, A. Mentalization in Children Exposed to Parental Methamphetamine Abuse: Relations to Children's Mental Health and Behavioral Outcomes. *Attach. Hum. Dev.* **2010**, *12*, 193-207.

(6) Center for Behavioral Health Statistics and Quality. (2016). Key Substance Use and Mental Health Indicators in the United States: Results from the 2015 National Survey on Drug Use and Health (HHS Publication No. SMA 16-4984, NSDUH Series H-51). Retrieved from http://www.samhsa.gov/data/ (accessed October 20, 2017).

(7) M, S.; Vasa, N. J.; Agarwal, V.; Chandapillai, J. UV Photo-ionization based Asymmetric Field Differential Ion Mobility Sensor for Trace Gas Detection. *Sens. Actuators B Chem.* **2014**, *195*, 44-51.

(8) Grabowska-Polanowska, B.; Faber, J.; Skowron, M.; Miarka, P.; Pietrzycka, A.; Śliwka, I.; Amann, A. Detection of Potential Chronic Kidney Disease Markers in Breath Using Gas Chromatography with Mass-spectral Setection Coupled with Thermal Desorption Method. *J. Chromatogr A* **2013,** *1301*, 179-189.

(9) Levitskaia, T. G.; Peterson, J. M.; Campbell, E. L.; Casella, A. J.; Peterman, D. R.; Bryan, S. A. Fourier Transform Infrared Spectroscopy and Multivariate Analysis for Online Monitoring of Dibutyl Phosphate Degradation Product in Tributyl Phosphate/n-Dodecane/Nitric Acid Solvent. *Ind. Eng. Chem. Res.* **2013,** *52*, 17607-17617.

(10) Krone, N.; Hughes, B. A.; Lavery, G. G.; Stewart, P. M.; Arlt, W.; Shackleton, C. H. L. Gas Chromatography/Mass Spectrometry (GC/MS) Remains a Pre-eminent Discovery Tool in Clinical Steroid Investigations Even in the Era of Fast Liquid Chromatography Tandem Mass Spectrometry (LC/MS/MS). *J. Steriod Biochem. Mol. Biol.* **2010,** *121*, 496-504.

(11) Hübschmann, H.-J., Fundamentals. In Handbook of GC-MS: Fundamentals and Applications; Wiley-VCH Verlag GmbH & Co. KGaA: Weinheim, 2015; pp 7-292.

(12) Yin Sun, K. Y. O., Detection Technologies for Chemical Warfare Agents and Toxic Vapors; CRC Press: Boca Raton, 2004; pp 112-133.

(13) Ewing, R. G.; Atkinson, D. A.; Eiceman, G. A.; Ewing, G. J. A Critical Review of Ion Mobility Spectrometry for the Detection of Explosives and Explosive Related Compounds. *Talanta* **2001**, *54,* 515-529.

(14) MacCrehan, W.; Moore, S.; Hancock, D. Development of SRM 2907 Trace Terrorist Explosives Simulants for the Detection of Semtex and Triacetone Triperoxide. *Anal. Chem.* **2011**, *83,* 9054-9059.

(15) Zolotov, Y. A. Ion Mobility Spectrometry. *J. Anal. Chem.* **2006,** *61,* 519-519.

(16) Mäkinen, M. A.; Anttalainen, O. A.; Sillanpää, M. E. T. Ion Mobility Spectrometry and Its Applications in Detection of Chemical Warfare Agents. *Anal. Chem.* **2010,** *82,* 9594-9600.

(17) Perr, J. M.; Furton, K. G.; Almirall, J. R. Solid Phase Microextraction Ion Mobility Spectrometer Interface for Explosive and Taggant Detection. *J. Sep. Sci.* **2005,** *28,* 177-183.

(18) Griffiths, P. R.; de Haseth, J. A. Other Components of FT-IR Spectrometers. In Fourier Transform Infrared Spectrometry; John Wiley & Sons, Inc.: New Jersey, 2006; pp 143-160.

(19) Toal, S. J.; Trogler, W. C. Polymer Sensors for Nitroaromatic Explosives Detection.

J. Mater. Chem. **2006,** *16*, 2871-2883.

(20) Chen, A.; Sun, H.; Pyayt, A.; Zhang, X.; Luo, J.; Jen, A.; Sullivan, P. A.; Elangovan, S.; Dalton, L. R.; Dinu, R.; Jin, D.; Huang, D. Chromophore-Containing Polymers for Trace Explosive Sensors. *J. Phys. Chem. C* **2008,** *112,* 8072-8078.

(21) Pramanik, S.; Zheng, C.; Zhang, X.; Emge, T. J.; Li, J. New Microporous Metal−Organic Framework Demonstrating Unique Selectivity for Detection of High Explosives and Aromatic Compounds. *J. Am. Chem. Soc.* **2011,** *133*, 4153-4155.

(22) Akhgari, F.; Fattahi, H.; Oskoei, Y. M. Recent Advances in Nanomaterial-based Sensors for Detection of Trace Nitroaromatic Explosives. *Sens. Actuators B Chem.* **2015,** *221*, 867-878.

(23) Salinas, Y.; Martinez-Manez, R.; Marcos, M. D.; Sancenon, F.; Costero, A. M.; Parra, M.; Gil, S. Optical Chemosensors and Reagents to Detect Explosives. *Chem. Soc. Rev.* **2012,** *41*, 1261-1296.

(24) Zhou, Q.; Swager, T. M. Fluorescent Chemosensors Based on Energy Migration in Conjugated Polymers: The Molecular Wire Approach to Increased Sensitivity. *J. Am. Chem. Soc.* **1995,** *117*, 12593-12602.

(25) Kwan, P. H.; MacLachlan, M. J.; Swager, T. M. Rotaxanated Conjugated Sensory Polymers. *J. Am. Chem. Soc.* **2004,** *126*, 8638-8639.

(26) Wosnick, J. H.; Mello, C. M.; Swager, T. M. Synthesis and Application of Poly(phenylene Ethynylene)s for Bioconjugation: A Conjugated Polymer-Based Fluorogenic Probe for Proteases. *J. Am. Chem. Soc.* **2005,** *127*, 3400-3405.

(27) Wosnick, J. H.; Liao, J. H.; Swager, T. M. Layer-by-Layer Poly(phenylene ethynylene) Films on Silica Microspheres for Enhanced Sensory Amplification. *Macromolecules* **2005,** *38*, 9287-9290.

(28) Yang, J.-S.; Swager, T. M. Porous Shape Persistent Fluorescent Polymer Films: An Approach to TNT Sensory Materials. *J. Am. Chem. Soc.* **1998,** *120*, 5321-5322.

(29) Esser, B.; Swager, T. M. Detection of Ethylene Gas by Fluorescence Turn-On of a Conjugated Polymer. *Angew. Chem. Int. Edit.* **2010,** *122*, 9056-9059.

(30) Sohn, H.; Calhoun, R. M.; Sailor, M. J.; Trogler, W. C. Detection of TNT and Picric Acid on Surfaces and in Seawater by Using Photoluminescent Polysiloles. *Angew. Chem. Int. Edit.* **2001,** *40*, 2104-2105.

(31) Toal, S. J.; Sanchez, J. C.; Dugan, R. E.; Trogler, W. C. Visual Detection of Trace Nitroaromatic Explosive Residue Using Photoluminescent Metallole-Containing Polymers. *J. Forensic Sci.* **2006,** *52*, 79-83.

(32) Sohn, H.; Sailor, M. J.; Magde, D.; Trogler, W. C. Detection of Nitroaromatic Explosives Based on Photoluminescent Polymers Containing Metalloles. *J. Am. Chem.*

Soc. **2003,** *125*, 3821-3830.

(33) Content, S.; Trogler, W. C.; Sailor, M. J. Detection of Nitrobenzene, DNT, and TNT Vapors by Quenching of Porous Silicon Photoluminescence. *Chem. Eur. J.* **2000,** *6,* 2205-2213.

(34) Li, H.; Wang, J.; Pan, Z.; Cui, L.; Xu, L.; Wang, R.; Song, Y.; Jiang, L. Amplifying Fluorescence Sensing Based on Inverse Opal Photonic Crystal Toward Trace TNT Detection. *J. Mater. Chem.* **2011,** *21,* 1730-1735.

(35) Guo, L.; Zu, B.; Yang, Z.; Cao, H.; Zheng, X.; Dou, X. APTS and RGO Co-Functionalized Pyrenated Fluorescent Nanonets for Representative Vapor Phase Nitroaromatic Explosives Detection. *Nanoscale* **2014,** *6,* 1467-1473.

(36) Adams, A. A.; Charles, P. T.; Deschamps, J. R.; Kusterbeck, A. W. Demonstration of Submersible High-Throughput Microfluidic Immunosensors for Underwater Explosives Detection. *Anal. Chem.* **2011,** *83,* 8411-8419.

(37) Gong, Y. N.; Jiang, L.; Lu, T. B. A Highly Stable Dynamic Fluorescent Metal-organic Framework for Selective Sensing of Nitroaromatic Explosives. *Chem. Commun.* **2013,** *49,* 1113-1115.

(38) Naddo, T.; Che, Y.; Zhang, W.; Balakrishnan, K.; Yang, X.; Yen, M.; Zhao, J.; Moore, J. S.; Zang, L. Detection of Explosives with a Fluorescent Nanofibril Film. *J. Am. Chem. Soc.* **2007,** *129,* 6978-6979.

(39) Zhang, C.; Che, Y.; Yang, X.; Bunes, B. R.; Zang, L. Organic Nanofibrils Based on Linear Carbazole Trimer for Explosive Sensing. *Chem. Commun.* **2010,** *46,* 5560-5562.

(40) Wen, D.; Fu, Y. Y.; Shi, L. Q.; He, C.; Dong, L.; Zhu, D. F.; He, Q. G.; Cao, H. M.; Cheng, J. G. Fine Structural Tuning of Fluorescent Copolymer Sensors for Methamphetamine Vapor Detection. *Sens. Actuators B Chem.* **2012,** *168,* 283-288.

(41) He, M.; Peng, H.; Wang, G.; Chang, X.; Miao, R.; Wang, W.; Fang, Y. Fabrication of a New Fluorescent Film and Its Superior Sensing Performance to N-methamphetamine in Vapor Phase. *Sens. Actuators B Chem.* **2016,** *227,* 255-262.

(42) Germain, M. E.; Knapp, M. J. Optical Explosives Detection: from Color Changes to Fluorescence Turn-on. *Chem. Soc. Rev.* **2009,** *38,* 2543-2555.

(43) Dasary, S. S. R.; Senapati, D.; Singh, A. K.; Anjaneyulu, Y.; Yu, H.; Ray, P. C. Highly Sensitive and Selective Dynamic Light-Scattering Assay for TNT Detection Using p-ATP Attached Gold Nanoparticle. *ACS Appl. Mater. Interfaces* **2010,** *2,* 3455-3460.

(44) Senesac, L.; Thundat, T. G. Nanosensors for Trace Explosive Detection. *Mater. Today* **2008,** *11,* 28-36.

(45) Lin, H.; Suslick, K. S. A. Colorimetric Sensor Array for Detection of Triacetone Triperoxide Vapor. *J. Am. Chem. Soc.* **2010,** *132,* 15519-15521.

(46) Zou, W.; Liu, W.; Luo, L.; Zhang, S.; Lu, R.; Veser, G. Detection of Nitro Explosives via LSPR Sensitive Silver Clusters Embedded in Porous Silica. *J. Mater. Chem.* **2012,** *22,* 12474-12478.

(47) Idros, N.; Ho, M.; Pivnenko, M.; Qasim, M.; Xu, H.; Gu, Z.; Chu, D. Colorimetric-Based Detection of TNT Explosives Using Functionalized Silica Nanoparticles. *Sensors* **2015,** *15,* 12891-12905.

(48) Peveler, W. J.; Roldan, A.; Hollingsworth, N.; Porter, M. J.; Parkin, I. P., Multichannel Detection and Differentiation of Explosives with a Quantum Dot Array. *ACS Nano* **2016,** *10,* 1139-1146.

(49) Fine, G. F.; Cavanagh, L. M.; Afonja, A.; Binions, R. Metal Oxide Semi-Conductor Gas Sensors in Environmental Monitoring. *Sensors* **2010,** *10,* 5469-5502.

(50) Wang, C.; Yin, L.; Zhang, L.; Xiang, D.; Gao, R. Metal Oxide Gas Sensors: Sensitivity and Influencing Factors. *Sensors* **2010,** *10,* 2088-2106.

(51) Brudzewski, K.; Osowski, S.; Pawlowski, W. Metal Oxide Sensor Arrays for Detection of Explosives at Sub-parts-per Million Concentration Levels by the Differential Electronic Nose. *Sens. Actuators B Chem.* **2012,** *161,* 528-533.

(52) Matzger, A. J.; Vaid, T. P.; Lewis, N. S. Vapor Sensing With Arrays of Carbon Black-Polymer Composites, Proceedings of SPIE, Orlando, United States, Aug 2, 1999, 3710. http://dx.doi.org/10.1117/12.357053 (accessed Oct 22, 2017).

(53) Che, Y.; Datar, A.; Yang, X.; Naddo, T.; Zhao, J.; Zang, L. Enhancing One-Dimensional Charge Transport through Intermolecular π-Electron Delocalization: Conductivity Improvement for Organic Nanobelts. *J. Am. Chem. Soc.* **2007,** *129,* 6354-6355.

(54) Che, Y.; Yang, X.; Liu, G.; Yu, C.; Ji, H.; Zuo, J.; Zhao, J.; Zang, L. Ultrathin N-type Organic Nanoribbons with High Photoconductivity and Application in Optoelectronic Vapor Sensing of Explosives. *J. Am. Chem. Soc.* **2010,** *132,* 5743-5750.

(55) Sharon, E.; Freeman, R.; Willner, I. Detection of Explosives Using Field-effect Transistors. *Electroanalysis* **2009,** *21,* 2185-2189.

(56) Engel, Y.; Elnathan, R.; Pevzner, A.; Davidi, G.; Flaxer, E.; Patolsky, F., Supersensitive detection of explosives by silicon nanowire arrays. *Angew. Chem. Int. Edit.* **2010,** *49,* 6830-6835.

(57) AlQahtani, H.; Sugden, M.; Puzzovio, D.; Hague, L.; Mullin, N.; Richardson, T.; Grell, M. Highly Sensitive Alkane Odour Sensors Based on Functionalised Gold Nanoparticles. *Sens. Actuators B Chem.* **2011,** *160,* 399-404.

(58) Seiyama, T.; Kato, A.; Fujiishi, K.; Nagatani, M. A New Detector for Gaseous Components Using Semiconductive Thin Films. *Anal. Chem.* **1962,** *34,* 1502-1503.

(59) Chen, S.; Slattum, P.; Wang, C.; Zang, L., Self-Assembly of Perylene Imide Molecules into 1D Nanostructures: Methods, Morphologies, and Applications. *Chem. Rev.* **2015,** *115,* 11967-11998.

(60) Dan, Y.; Lu, Y.; Kybert, N. J.; Luo, Z.; Johnson, A. T. C. Intrinsic Response of Graphene Vapor Sensors. *Nano Lett.* **2009,** *9,* 1472-1475.

(61) Perkins, F. K.; Friedman, A. L.; Cobas, E.; Campbell, P. M.; Jernigan, G. G.; Jonker, B. T. Chemical Vapor Sensing with Monolayer MoS2. *Nano Lett.* **2013,** *13,* 668-673.

(62) Strle, D.; Štefane, B.; Zupanič, E.; Trifkovič, M.; Maček, M.; Jakša, G.; Kvasič, I.; Muševič, I. Sensitivity Comparison of Vapor Trace Detection of Explosives Based on Chemo-Mechanical Sensing with Optical Detection and Capacitive Sensing with Electronic Detection. *Sensors* **2014,** *14,* 11467.

(63) Ruan, W.; Li, Y.; Tan, Z.; Liu, L.; Jiang, K.; Wang, Z., In Situ Synthesized Carbon Nanotube Networks on a Microcantilever for Sensitive Detection of Explosive Vapors. *Sens. Actuators B Chem.* **2013,** *176,* 141-148.

(64) Afzal, A.; Iqbal, N.; Mujahid, A.; Schirhagl, R. Advanced Vapor Recognition Materials for Selective and Fast Responsive Surface Acoustic Wave Sensors: A Review. *Anal. Chim. Acta* **2013,** *787,* 36-49.

(65) Deyi, K.; Tao, M.; Yongchun, T.; Lin, N.; Tao, Z.; Wei, L.; Zhengyong, Z.; Rui, W. A MEMS Sensor Array for Explosive Particle Detection, Proceedings of the International Conference on Information Acquisition, Hefei, China, June 21-25, 2004; pp 278-28.

(66) Liu, S.; Ponrathnam, T.; Sun, H.; Nagarajan, R.; Kumar, J.; Gu, Z.; Kurup, P. Detection of Explosive Vapors by Surface Acoustic Wave Sensors Containing Novel Siloxane Based Coatings. *J. Macromol. Sci. Pure Appl. Chem.* **2010,** *47,* 1172-1175.

(67) Robinson, J. T.; Perkins, F. K.; Snow, E. S.; Wei, Z.; Sheehan, P. E. Reduced Graphene Oxide Molecular Sensors. *Nano Lett.* **2008,** *8,* 3137-3140.

(68) Compton, O. C.; Nguyen, S. T. Graphene Oxide, Highly Reduced Graphene Oxide, and Graphene: Versatile Building Blocks for Carbon-Based Materials. *Small* **2010,** *6,* 711-723.

(69) Kalantar-zadeh, K.; Ou, J. Z. Biosensors Based on Two-Dimensional MoS2. *ACS Sensors* **2016,** *1,* 5-16.

(70) Kauffman, D. R.; Star, A. Graphene Versus Carbon Nanotubes for Chemical Sensor and Fuel Cell Applications. *Analyst* **2010,** *135,* 2790-2797.

(71) Iijima, S. Helical Microtubules of Graphitic Carbon. *Nature* **1991,** *354,* 56-58.

(72) Iijima, S.; Ichihashi, T. Single-shell Carbon Nanotubes of 1-nm Diameter. *Nature* **1993,** *363,* 603-605.

(73) Iijima, S. Carbon Nanotubes: Past, Present, and Future. *Phys. B Condens. Matter* **2002,** *323,* 1-5.

(74) Samanta, S. K.; Fritsch, M.; Scherf, U.; Gomulya, W.; Bisri, S. Z.; Loi, M. A. Conjugated Polymer-Assisted Dispersion of Single-Wall Carbon Nanotubes: The Power of Polymer Wrapping. *Acc. Chem. Res.* **2014,** *47,* 2446-2456.

(75) Dresselhaus, M. S., Dresselhaus, G., Avouris, P. Nanotube Growth and Characterization. Carbon Nanotubes: Synthesis, Structure, Properties and Applications; Springer-Verlag Berlin Heidelberg New York, 2001; pp 11-28.

(76) Shi, Z.; Lian, Y.; Liao, F. H.; Zhou, X.; Gu, Z.; Zhang, Y.; Iijima, S.; Li, H.; Yue, K. T.; Zhang, S.-L. Large Scale Synthesis of Single-wall Carbon Nanotubes by Arc-discharge Method. *J. Phys. Chem. Solid* **2000,** *61,* 1031-1036.

(77) Hutchison, J. L.; Kiselev, N. A.; Krinichnaya, E. P.; Krestinin, A. V.; Loutfy, R. O.; Morawsky, A. P.; Muradyan, V. E.; Obraztsova, E. D.; Sloan, J.; Terekhov, S. V.; Zakharov, D. N. Double-walled Carbon Nanotubes Fabricated by a Hydrogen Arc Discharge Method. *Carbon* **2001,** *39,* 761-770.

(78) Vander Wal , R. L.; Berger , G. M.; Ticich , T. M. Carbon Nanotube Synthesis in a Flame Using Laser Ablation for In Situ Catalyst Generation. *Appl. Phys. Mater. Sci. Process* **2003,** *77,* 885-889.

(79) Yudasaka, M.; Komatsu, T.; Ichihashi, T.; Iijima, S. Single-wall Carbon Nanotube Formation by Laser Ablation using Double-targets of Carbon and Metal. *Chem. Phys. Lett.* **1997,** *278,* 102-106.

(80) Chiang, I. W.; Brinson, B. E.; Huang, A. Y.; Willis, P. A.; Bronikowski, M. J.; Margrave, J. L.; Smalley, R. E.; Hauge, R. H. Purification and Characterization of Single-Wall Carbon Nanotubes (SWNTs) Obtained from the Gas-Phase Decomposition of CO (HiPco Process). *J. Phys. Chem. B* **2001,** *105,* 8297-8301.

(81) Nikolaev, P.; Bronikowski, M. J.; Bradley, R. K.; Rohmund, F.; Colbert, D. T.; Smith, K. A.; Smalley, R. E. Gas-phase Catalytic Growth of Single-walled Carbon Nanotubes from Carbon Monoxide. *Chem. Phys. Lett.* **1999,** *313,* 91-97.

(82) O'Connell, M. J.; Bachilo, S. M.; Huffman, C. B.; Moore, V. C.; Strano, M. S.; Haroz, E. H.; Rialon, K. L.; Boul, P. J.; Noon, W. H.; Kittrell, C.; Ma, J.; Hauge, R. H.; Weisman, R. B.; Smalley, R. E. Band Gap Fluorescence from Individual Single-Walled Carbon Nanotubes. *Science* **2002,** *297,* 593-596.

(83) Sohrabi, B.; Poorgholami-Bejarpasi, N.; Nayeri, N. Dispersion of Carbon Nanotubes Using Mixed Surfactants: Experimental and Molecular Dynamics Simulation Studies. The *J. Phys. Chem. B* **2014,** *118,* 3094-3103.

(84) Zhang, Z.; Che, Y.; Smaldone, R. A.; Xu, M.; Bunes, B. R.; Moore, J. S.; Zang, L. Reversible Dispersion and Release of Carbon Nanotubes Using Foldable Oligomers. *J. Am. Chem. Soc.* **2010,** *132,* 14113-14117.

(85) Lee, H. W.; Yoon, Y.; Park, S.; Oh, J. H.; Hong, S.; Liyanage, L. S.; Wang, H.; Morishita, S.; Patil, N.; Park, Y. J.; Park, J. J.; Spakowitz, A.; Galli, G.; Gygi, F.; Wong, P. H. S.; Tok, J. B. H.; Kim, J. M.; Bao, Z. Selective Dispersion of High Purity Semiconducting Single-walled Carbon Nanotubes with Regioregular Poly(3-alkylthiophene)s. *Nat. Commun.* **2011,** *2,* 541.

(86) Zou, J.; Liu, L.; Chen, H.; Khondaker, S. I.; McCullough, R. D.; Huo, Q.; Zhai, L. Dispersion of Pristine Carbon Nanotubes Using Conjugated Block Copolymers. *Adv. Mater.* **2008,** *20,* 2055-2060.

(87) Bluemmel, P.; Setaro, A.; Popeney, C. S.; Haag, R.; Reich, S. Dispersion of Carbon Nanotubes Using an Azobenzene Derivative. *Phys. Status Solidi B* **2010,** *247,* 2891-2894.

(88) Zheng, M.; Jagota, A.; Semke, E. D.; Diner, B. A.; McLean, R. S.; Lustig, S. R.; Richardson, R. E.; Tassi, N. G. DNA-assisted Dispersion and Separation of Carbon Nanotubes. *Nat. Mater.* **2003,** *2,* 338-342.

(89) Quan-Hong, Y.; Qi, W.; Nittaya, G.; Claudio, J. O.; Lan, C.; Iris, S. N.; Zhenping, Z.; Zhiyuan, T.; Tom, B.; Wei, H. L. Loosening the DNA Wrapping Around Single-walled Carbon Nanotubes by Increasing the Strand Length. *Nanotechnology* **2009,** *20,* 195603.

(90) Zhang, Y.; Bunes, B. R.; Wang, C.; Wu, N.; Zang, L. Poly(3-alkylthiophene)/CNT-Based Chemiresistive Sensors for Vapor Detection of Linear Alkanes: Effect of Polymer Side Chain Length. *Sens. Actuators B Chem.* **2017,** *247,* 713-717.

(91) Berton, N.; Lemasson, F.; Hennrich, F.; Kappes, M. M.; Mayor, M. Influence of Molecular Weight on Selective Oligomer-assisted Dispersion of Single-walled Carbon Nannotubes and Subsequent Polymer Exchange. *Chem. Commun.* **2012,** *48,* 2516-8.

(92) Lemasson, F. A.; Strunk, T.; Gerstel, P.; Hennrich, F.; Lebedkin, S.; Barner-Kowollik, C.; Wenzel, W.; Kappes, M. M.; Mayor, M. Selective Dispersion of Single-Walled Carbon Nanotubes with Specific Chiral Indices by Poly(N-decyl-2,7-carbazole). *J. Am. Chem. Soc.* **2011,** *133,* 652-655.

(93) Nish, A.; Hwang, J.-Y.; Doig, J.; Nicholas, R. J. Highly Selective Dispersion of Single-walled Carbon Nanotubes using Aromatic Polymers. *Nat. Nanotechnol.* **2007,** *2,* 640-646.

(94) Kong, J.; Franklin, N. R.; Zhou, C.; Chapline, M. G.; Peng, S.; Cho, K.; Dai, H. Nanotube Molecular Wires as Chemical Sensors. *Science* **2000,** *287,* 622-625.

(95) Collins, P. G.; Bradley, K.; Ishigami, M.; Zettl, A. Extreme Oxygen Sensitivity of Electronic Properties of Carbon Nanotubes. *Science* **2000,** *287,* 1801-1804.

(96) Bondavalli, P.; Legagneux, P.; Pribat, D. Carbon Nanotubes Based Transistors as Gas Sensors: State of the Art and Critical Review. *Sens Actuators B Chem.* **2009,** *140,* 304-318.

(97) Chen, P.-C.; Sukcharoenchoke, S.; Ryu, K.; Gomez de Arco, L.; Badmaev, A.; Wang, C.; Zhou, C. 2,4,6-Trinitrotoluene (TNT) Chemical Sensing Based on Aligned Single-

Walled Carbon Nanotubes and ZnO Nanowires. *Adv. Mater.* **2010,** *22,* 1900-1904.

(98) Chen, R. J.; Franklin, N. R.; Kong, J.; Cao, J.; Tombler, T. W.; Zhang, Y.; Dai, H. Molecular Photodesorption from Single-walled Carbon Nanotubes. *Appl. Phys. Lett.* **2001,** *79,* 2258-2260.

(99) Chen, G.; Paronyan, T. M.; Pigos, E. M.; Harutyunyan, A. R. Enhanced Gas Sensing in Pristine Carbon Nanotubes under Continuous Ultraviolet Light Illumination. *Sci. Rep.* **2012,** *2,* 343.

(100) Banerjee, S.; Hemraj-Benny, T.; Wong, S. S. Covalent Surface Chemistry of Single-walled Carbon Nanotubes. *Adv. Mater.* **2005,** *17,* 17-29.

(101) Peng, X.; Wong, S. S. Functional Covalent Chemistry of Carbon Nanotube Surfaces. *Adv. Mater.* **2009,** *21,* 625-642.

(102) Peng, X.; Sfeir, M. Y.; Zhang, F.; Misewich, J. A.; Wong, S. S. Covalent Synthesis and Optical Characterization of Double-Walled Carbon Nanotube-Nanocrystal Heterostructures. *J. Phys. Chem. C* **2010,** *114,* 8766-8773.

(103) Huang, J.; Ng, A. L.; Piao, Y.; Chen, C.-F.; Green, A. A.; Sun, C.-F.; Hersam, M. C.; Lee, C. S.; Wang, Y. Covalently Functionalized Double-Walled Carbon Nanotubes Combine High Sensitivity and Selectivity in the Electrical Detection of Small Molecules. *J. Am. Chem. Soc.* **2013,** *135,* 2306-2312.

(104) Wang, F.; Swager, T. M. Diverse Chemiresistors Based upon Covalently Modified Multiwalled Carbon Nanotubes. *J. Am. Chem. Soc.* **2011,** *133,* 11181-11193.

(105) Schnorr, J. M.; Van Der Zwaag, D.; Walish, J. J.; Weizmann, Y.; Swager, T. M. Sensory Arrays of Covalently Functionalized Single-walled Carbon Nanotubes for Explosive Detection. *Adv. Funct. Mater.* **2013,** *23,* 5285-5291.

(106) Liu, Y.; Chen, C. L.; Zhang, Y.; Sonkusale, S. R.; Wang, M. L.; Dokmeci, M. R. SWNT based Nanosensors for Wireless Detection of Explosives and Chemical Warfare Agents. *IEEE Sens. J.* **2013,** *13,* 202-210.

(107) Kybert, N. J.; Lerner, M. B.; Yodh, J. S.; Preti, G.; Johnson, A. T. C. Differentiation of Complex Vapor Mixtures Using Versatile DNA–Carbon Nanotube Chemical Sensor Arrays. *ACS Nano* **2013,** *7,* 2800-2807.

(108) Heller, D. A.; Pratt, G. W.; Zhang, J.; Nair, N.; Hansborough, A. J.; Boghossian, A. A.; Reuel, N. F.; Barone, P. W.; Strano, M. S. Peptide Secondary Structure Modulates Single-walled Carbon Nanotube Fluorescence as a Chaperone Sensor for Nitroaromatics. *Proc. Natl. Acad. Sci. U.S.A.* **2011,** *108,* 8544-8549.

(109) Park, M.; Cella, L. N.; Chen, W.; Myung, N. V.; Mulchandani, A. Carbon Nanotubes-based Chemiresistive Immunosensor for Small Molecules: Detection of Nitroaromatic Explosives. *Biosens. Bioelectron.* **2010,** *26,* 1297-1301.

(110) Qi, P.; Vermesh, O.; Grecu, M.; Javey, A.; Wang, Q.; Dai, H.; Peng, S.; Cho, K. J. Toward Large Arrays of Multiplex Functionalized Carbon Nanotube Sensors for Highly Sensitive and Selective Molecular Detection. *Nano Lett.* **2003,** *3,* 347-351.

(111) An, K. H.; Jeong, S. Y.; Hwang, H. R.; Lee, Y. H. Enhanced Sensitivity of a Gas Sensor Incorporating Single-Walled Carbon Nanotube–Polypyrrole Nanocomposites. *Adv. Mater.* **2004,** *16,* 1005-1009.

(112) Wang, F.; Yang, Y.; Swager, T. M. Molecular Recognition for High Selectivity in Carbon Nanotube/Polythiophene Chemiresistors. *Angew. Chem. Int. Edit*. **2008,** *47,* 8394-8396.

(113) Ding, M.; Tang, Y.; Gou, P.; Reber, M. J.; Star, A. Chemical Sensing with Polyaniline Coated Single-Walled Carbon Nanotubes. *Adv. Mater.* **2011,** *23,* 536-540.

(114) Lu, Y.; Meyyappan, M.; Li, J. Trace Detection of Hydrogen Peroxide Vapor Using a Carbon-Nanotube-Based Chemical Sensor. *Small* **2011,** *7,* 1714-1718.

(115) Ishihara, S.; Azzarelli, J. M.; Krikorian, M.; Swager, T. M. Ultratrace Detection of Toxic Chemicals: Triggered Disassembly of Supramolecular Nanotube Wrappers. *J. Am. Chem.* Soc. **2016,** *138,* 8221-8227.

(116) Kim, T. H.; Lee, B. Y.; Jaworski, J.; Yokoyama, K.; Chung, W.-J.; Wang, E.; Hong, S.; Majumdar, A.; Lee, S.-W. Selective and Sensitive TNT Sensors Using Biomimetic Polydiacetylene-Coated CNT-FETs. *ACS Nano* **2011,** *5,* 2824-2830.

(117) Zhang, Y.; Xu, M.; Bunes, B. R.; Wu, N.; Gross, D. E.; Moore, J. S.; Zang, L. Oligomer-Coated Carbon Nanotube Chemiresistive Sensors for Selective Detection of Nitroaromatic Explosives. *ACS Appl. Mater. Interfaces* **2015,** 7*,* 7471-7475.

(118) Lu, X.; Quan, Y.; Xue, Z.; Wu, B.; Qi, H.; Liu, D. Determination of Explosives based on Novel type of Sensor Using Porphyrin Functionalized Carbon Nanotubes. *Colloids Surf B Biointerfaces* **2011,** *88,* 396-401.

(119) Frazier, K. M.; Swager, T. M. Robust Cyclohexanone Selective Chemiresistors Based on Single-Walled Carbon Nanotubes. *Anal. Chem.* **2013,** *85,* 7154-7158.

(120) Wei, L.; Lu, D.; Wang, J.; Wei, H.; Zhao, J.; Geng, H.; Zhang, Y. Highly Sensitive Detection of Trinitrotoluene in Water by Chemiresistive Sensor based on Noncovalently Amino Functionalized Single-walled Carbon Nanotube. *Sens. Actuators B Chem.* **2014,** *190,* 529-534.

(121) Snow, E. S.; Perkins, F. K.; Houser, E. J.; Badescu, S. C.; Reinecke, T. L. Chemical Detection with a Single-Walled Carbon Nanotube Capacitor. *Science* **2005,** *307,* 1942-1945.

(122) Evans, G. P.; Buckley, D. J.; Skipper, N. T.; Parkin, I. P. Single-walled Carbon Nanotube Composite Inks for Printed Gas Sensors: Enhanced detection of NO2, NH3, EtOH and acetone. *RSC Adv.* **2014,** *4,* 51395-51403.

(123) Buck, L. B. Unraveling the Sense of Smell (Nobel Lecture). *Angew. Chem. Int. Edit.* **2005,** *44,* 6128-6140.

(124) Albert, K. J.; Lewis, N. S.; Schauer, C. L.; Sotzing, G. A.; Stitzel, S. E.; Vaid, T. P.; Walt, D. R. Cross-Reactive Chemical Sensor Arrays. *Chem. Rev.* **2000,** *100,* 2595-2626.

(125) Chen, P. C.; Ishikawa, F. N.; Chang, H. K.; Ryu, K.; Zhou, C. A Nanoelectronic Nose: A Hybrid Nanowire/Carbon Nanotube Sensor Array with Integrated Micromachined Hotplates for Sensitive Gas Discrimination. *Nanotechnology* **2009,** *20,* 125503.

(126) Lonergan, M. C.; Severin, E. J.; Doleman, B. J.; Beaber, S. A.; Grubbs, R. H.; Lewis, N. S. Array-Based Vapor Sensing Using Chemically Sensitive, Carbon Black−Polymer Resistors. *Chem. Mater.* **1996,** *8,* 2298-2312.

(127) Gao, T.; Tillman, E. S.; Lewis, N. S. Detection and Classification of Volatile Organic Amines and Carboxylic Acids Using Arrays of Carbon Black-Dendrimer Composite Vapor Detectors. *Chem. Mater.* **2005,** *17,* 2904-2911.

(128) Gao, T.; Woodka, M. D.; Brunschwig, B. S.; Lewis, N. S. Chemiresistors for Array-Based Vapor Sensing Using Composites of Carbon Black with Low Volatility Organic Molecules. *Chem. Mater.* **2006,** *18,* 5193-5202.

(129) Jurs, P. C.; Bakken, G. A.; McClelland, H. E. Computational Methods for the Analysis of Chemical Sensor Array Data from Volatile Analytes. *Chem. Rev.* **2000,** *100,* 2649-2678.

(130) Wang, B.; Cancilla, J. C.; Torrecilla, J. S.; Haick, H. Artificial Sensing Intelligence with Silicon Nanowires for Ultraselective Detection in the Gas Phase. *Nano Lett.* **2014,** *14,* 933-938.

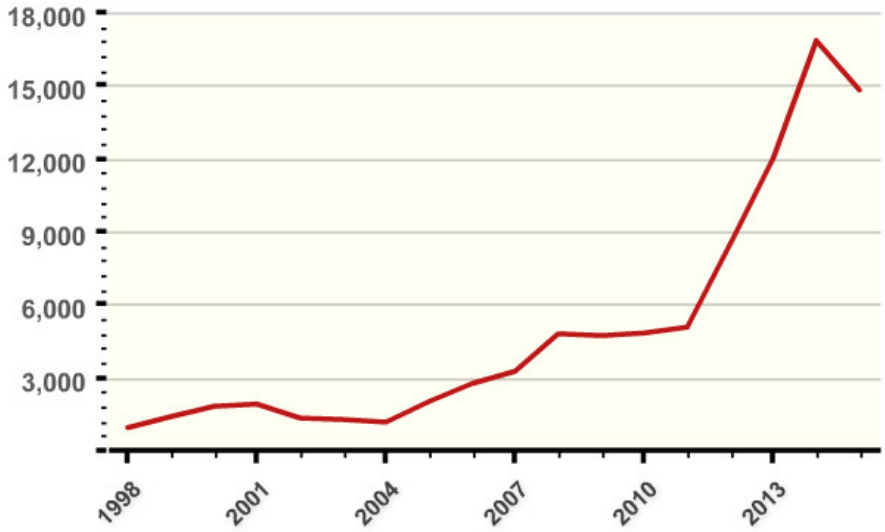

Figure 1.1 Total number of terrorism incidents worldwide in recent years. (National Consortium for the Study of Terrorism and Responses to Terrorism (START). (2017). Global Terrorism Database [Data file]. Retrieved from https://www.start.umd.edu/gtd)

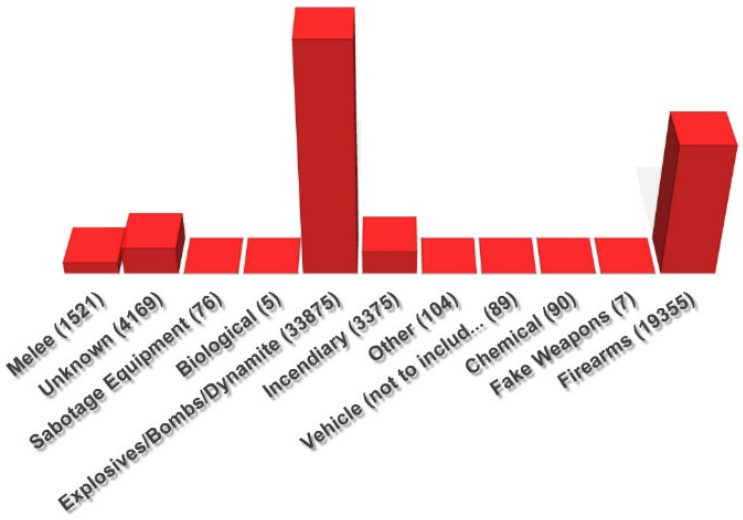

Figure 1.2 Bar plot of the types of terrorism incidents worldwide. (National Consortium for the Study of Terrorism and Responses to Terrorism (START). (2017). Global Terrorism Database [Data file]. Retrieved from https://www.start.umd.edu/gtd)

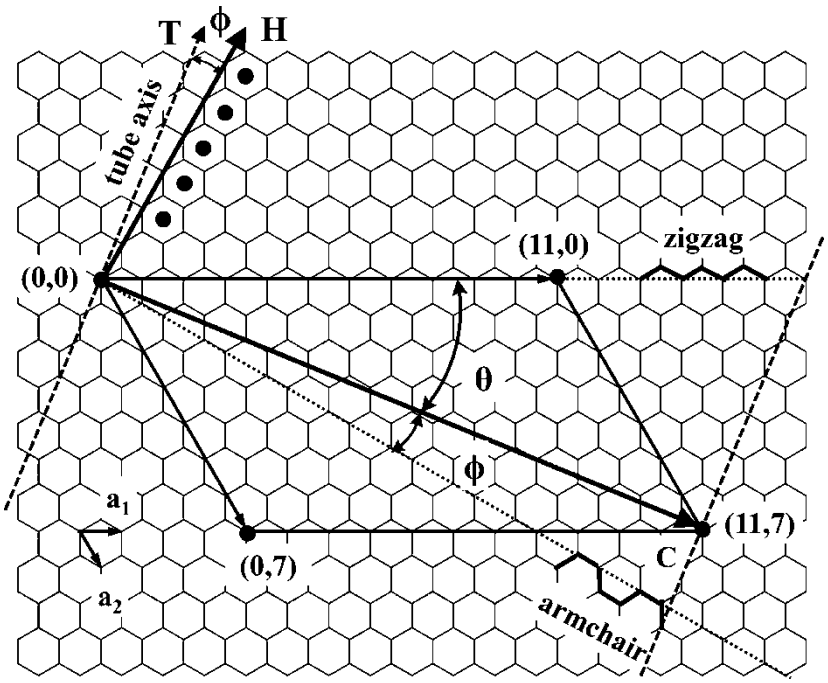

Figure 1.3 Building of carbon nanotubes from graphene sheets. (Adapted from (74)).

CHAPTER 2

OLIGOMER-COATED CARBON NANOTUBE CHEMIRESISTIVE SENSORS FOR SELECTIVE DETECTION OF NITROAROMATIC EXPLOSIVES[1]

2.1 Abstract

High-performance chemiresistive sensors were made using a porous thin film of single-walled carbon nanotubes (CNTs) coated with a carbazolylethynylene (Tg-Car) oligomer for trace vapor detection of nitroaromatic explosives. The sensors detect low concentrations of 4-nitrotoluene (NT), 2,4,6-trinitrotoluene (TNT), and 2,4-dinitrotoluene (DNT) vapors at ppb to ppt levels. The sensors also show high selectivity to NT from other common organic reagents at significantly higher vapor concentrations. Furthermore, by using Tg-Car/CNT sensors and uncoated CNT sensors in parallel, differential sensing of NT, TNT, and DNT vapors was achieved. This work provides a methodology to create selective CNT-based sensors and sensor arrays.

---

[1] Adapted with permission from Zhang, Y.; Xu, M.; Bunes, B. R.; Wu, N.; Gross, E. D.; Zang, L. Oligomer-Coated Carbon Nanotube Chemiresistive Sensors for Selective Detection of Nitroaromatic Explosives. *ACS Appl. Mater. Interfaces* **2015**, *7*, 7471-7475.

2.2 Introduction

A low-cost, portable, and sensitive sensor for explosive compounds can provide great benefits to homeland security, military operations, and environmental safety (1-4). Nitroaromatic (NA) explosive compounds, such as 2,4,6-trinitrotoluene (TNT) and 2,4-dinitrotoluene (DNT), are among the most common explosives in the world. Several detection technologies have been developed. Although traditional analytical methods like gas chromatography-mass spectrometry (5) and ion mobility spectrometry (6) afford accurate measurements, they require sophisticated and expensive instruments, which limits their usage. NA explosive sensors based on fluorescence materials (7-9), especially carbazole-based polymers (10) or oligomers (10-14), provide easy, sensitive detection of NA explosives. Yet, fluorescence-based sensors involve optical excitation and monitoring, which require precise alignment and calibration. Chemical sensors based on field-effect transistors using functionalized one-dimensional semiconducting materials (3, 15) (e.g., metal oxide nanowires, silicon nanowires, and carbon nanotubes) have attracted much attention because of their high sensitivity and simple integration with circuits. However, their applications have been limited by complicated fabrication processes arising from factors including a lack of solubility of the nanomaterials. Moreover, metal oxides and other inorganic sensor materials demonstrate significant response to water vapor (humidity), causing false positives.

Chemiresistive sensor systems based on carbon nanotubes (CNTs) are easy to fabricate, small in size, and highly sensitive (16-17). However, their use has been limited to the lab scale because of difficulties in dispersing CNTs and poor sensor selectivity. Researchers have explored both covalent (18) and noncovalent (4), (18-19) modification to solve these problems. Although covalent modifications are robust, they usually alter the electric

properties of the CNT significantly and require complicated organic synthesis (21). Noncovalent modifications provide a wide range of materials to choose from without changing the CNT's band structure (22). We report herein the demonstration of a NA explosive sensor using single-walled CNTs noncovalently functionalized with a carbazolylethynylene oligomer (Tg-Car, see Figure 2.1a for the structure). There are three key features of our design. (1) The Tg-Car oligomer greatly enhances the dispersion of CNTs in organic solvents and thus facilitates the fabrication of an unbundled, uniform, and porous thin film using a very simple drop-casting method. The porous surface of Tg-Car/CNT composite also aids in vapor diffusion, which enhances the vapor detection efficiency. (2) The noncovalent modification not only maintains the electron transport properties of CNTs, but also improves the selectivity of the sensors to NA explosive compounds. Moreover, by adding a separate channel of the uncoated CNT sensors as a reference, we can both distinguish NAs from potential interferences and differentiate three different NAs compounds from each other. (3) The insulating oligomer coating creates charge carrier tunnel barriers at the junctions of the CNT network. Swelling of the oligomer due to exposure to an analyte decreases the conductivity of the CNT network by increasing the tunneling distance. Meanwhile, the carbazole building block of the Tg-Car oligomer is very similar to previously reported fluorescence sensing materials (11-14), which were also based on the carbazole structure and demonstrated strong binding affinity and selectivity for NA explosives.

2.3 Results and Discussion

The CNTs were dispersed following a process previously developed in our lab (22-23). Briefly, CNTs were added into a chloroform solution containing an excess amount of Tg-

Car oligomer, followed by sonication. The synthetic details of the Tg-Car oligomer can be found in our previous work (24). Aggregates were removed by three iterations of centrifugation. Finally, a uniform and stable Tg-Car/CNT suspension in chloroform was obtained (shown in the left vial in Figure 2.1b). The suspension was stable for over three years without precipitation while the uncoated CNTs in chloroform aggregated within min after sonication (shown in the right vial Figure 2.1b). This demonstrates an improvement in solubility, which makes the device fabrication process facile and reproducible. Then, 2-6 μL (2 μL at a time) of the diluted Tg-Car/CNT suspension was drop-cast on a chip with pre-patterned interdigitated electrode pairs (IDEs) until the resistance was within the range of 50 kΩ to 200 kΩ. The device was heated to 80 °C for 5 min in an ambient environment to remove the remaining chloroform. Figure 2.1c shows the schematic view of the sensor. The morphology of the thin film was studied by atomic force microscopy (AFM) (Figure 2.1d) directly after fabrication. The AFM image indicates that a porous, bundle-free thin film was formed. The fibril materials in the thin film are individually separated CNTs coated with a layer of Tg-Car oligomer (see the black arrows in Figure 2.1d). An AFM image showing the surface morphology of a larger area is provided in Figure 2.2. This continuous, porous surface of these devices allows diffusion of analyte molecules into the thin film, which facilitates vapor detection.

To evaluate of the sensory performance of the Tg-Car/CNT devices, we first tested the vapor of 4-nitrotoluene (NT), which is commonly used as a taggant in NA explosive materials. It is relatively easy to accurately dilute and deliver NT vapor with our vapor generation system (see Figure 2.3, for detail) because its saturated vapor pressure at room temperature is much higher than TNT and DNT. The vapor generation system consists of a diluting stream of dry air at a constant flow rate of 100 sccm (standard cubic centimeter

per minute). To this stream of dry air, a known volume of saturated vapor was infused by a programmable syringe pump. The saturated vapor of each analyte was generated in a 60 mL glass syringe and allowed to equilibrate for 2 h at room temperature. The diluted vapor was then delivered into a custom PTFE enclosure, in which the sensors were contained. The sensory response to the exposure of an analyte is defined as the relative conductivity change of the sensor before and after the exposure. The sensors were operated at a constant bias voltage of 1.0 V. Figure 2.4a shows the baseline-corrected response of the Tg-Car/CNT sensor to 1.5, 2.0, and 3.0 ppm of NT vapor, which were diluted from 3, 4 and 6 sccm streams of the saturated vapor of NT (25). The original data plot without baseline correction shown in Figure 2.5. Overall, the sensor's response is fast and recoverable. A limit of detection (LOD) of 95 ppb is calculated based on a linear fitting of the data following a method reported in literature (26).

The sensor's ability to discriminate between NT and common reagents, such as acetone, ethanol, hexane, methanol, toluene, and water, was investigated. These common reagents were diluted to about 1% of the saturated vapor at room temperature (1 sccm of saturated vapor diluted with 100 sccm of dry air) and delivery to the sensor. Figure 2.6 shows the conductance change of the Tg-Car/CNT sensor in response to the vapors of these common reagents. The selectivity of the sensor to NT is good considering that the other vapors are at concentrations 2-3 orders of magnitudes higher than that of NT while the sensory response to NT is significantly lower. Moreover, the sensor shows a minimal response to water vapor, which indicates robustness against humidity.

Next, we compared the vapor detection performance of the Tg-Car/CNT sensors with uncoated CNT sensors, similar to those reported previously. (15, 17) The uncoated CNT sensors were fabricated from a CNT/dimethylformamide (DMF) suspension. Figure 2.7a

shows the results from both sensors in response to NT (7 ppm), DNT (36 ppb) and TNT (0.7 ppb) diluted from 15 sccm of saturated vapors at room temperature. The sensory response of the Tg-Car/CNT sensors and uncoated CNT sensors were monitored simultaneously and the real-time results are provided in the Figure 2.8. The uncoated CNT sensor shows an increase of conductance to all the analytes while the Tg-Car/CNT sensor shows an opposite response trend. This is reasonable because uncoated CNTs are p-type materials with holes as the major charge carriers and the conductivity is expected increase when exposed to electron-withdrawing analytes such as NA explosive compounds. For instance, even though the concentration of DNT is about 200 times lower than the concentration of NT, the sensory response is higher for DNT. This is mainly because the electron-withdrawing ability of DNT is higher than that of NT. For the Tg-Car/CNT sensor, the conductivity decreases upon exposure. To account for this decrease, we propose a sensing mechanism based on the swelling of the Tg-Car oligomer between adjacent CNTs, rather than charge transfer. This mechanism will be discussed in detail later.

There are significant research interests regarding the differential detection of NT, DNT, and TNT, as the chemical structures and properties of these compounds are so similar. One possible solution is to use sensor arrays (27) that incorporate multiple sensors in one detection system. We built a simple array using the Tg-Car/CNT sensors and uncoated CNT sensors. Figure 2.7b shows a scatter plot of the sensory response from the Tg-Car/CNT sensor and the uncoated CNT sensor to vapors of NT (4, 7, and 12 ppm), DNT (23, 36, and 63 ppb), and TNT (0.4, 0.7, and 1.3 ppb). As it is clearly shown, the cluster of data points for NT is far away from the clusters of data points for DNT and TNT, which

means it can be distinguished from the other NA compounds. The clusters of DNT and TNT are closer but still separate. This result demonstrates that by using a simple array of just two sensor components, DNT and TNT can be selectively detected in this range of concentrations. The sensory response of Tg-Car/CNT is nearly saturated at higher concentrations of DNT and TNT (see Figure 2.7b). This may be due to the strong electron donor-acceptor interaction between these compounds and the carbazole units in Tg-Car oligomer. The noncovalent modification of CNTs not only simplifies the device fabrication, but also demonstrates a practical way to improve the selectivity of the CNT sensors through the choice of monomer building blocks.

The mechanism of the Tg-Car/CNT sensors is different from the charge-transfer mechanism mentioned in previous reports (28) and in the uncoated CNT sensors used in this work. We propose that the mechanism of the Tg-Car/CNT sensors is due to the swelling of the Tg-Car/CNT thin film (shown in Scheme 2.1), which is similar to previously reported carbon-black/polymer (29) or carbon-black/small-molecule (29-30) chemical sensors. In the Tg-Car/CNT sensors, the conductivity of the thin film is from the CNT network. However, the junctions between CNTs are separated by the insulating Tg-Car oligomer. When voltage is applied between source and drain, the charge carriers (holes) in the CNT network tunnel through the interfaces formed by the Tg-Car oligomer. When the sensor is exposed to an analyte, the Tg-Car oligomer swells and the distance separated by the oligomer increases; thus, the tunnel barrier in the CNT network increases. As a result, the conductivity of the sensor decreases. However, the sensing performance from our Tg-Car/CNT sensors to the NA explosive compounds is significantly enhanced compared to the previous carbon-black swelling-based NA sensors (30) because of the

following reasons. First, the porosity in our sensors is high. This is important for vapor sensors because it greatly enhances the surface area available for interaction with the analyte. Meanwhile, we can disperse CNTs using a relatively small amount of Tg-Car oligomer. For most of the previous carbon-black swelling-based sensors (29-30), carbon-black was immersed in a large volume of polymer or small molecule with limited open surface area, which decreases the sensitivity. Second, the Tg-Car oligomer provides a strong affinity to NA explosive compounds, which helps the sensor respond at low concentrations and improves the selectivity of the sensor from other common chemical reagents (as shown by the results in Figures 2.6 and 2.7).

2.4 Conclusion

In summary, we have fabricated a Tg-Car/CNT composite sensor using a very simple drop-casting method. The sensor shows high sensitivity to NA explosive compounds and also shows high selectivity among other common organic reagents. The combination of uncoated CNT sensor with the Tg-Car/CNT sensor provides differential sensing between the three NA explosive compounds. The work demonstrates the use of a carbazole oligomer and CNT composite materials for a simple chemiresistive sensor with high sensitivity, which can be easily integrated into sensor arrays to achieve differential sensing.

2.5 Experimental Methods and Materials

2.5.1 Materials and General Instruments

Carbon nanotubes (SG65i, single walled, >95% semiconducting species) were purchased from SouthWest NanoTechnologies. Carbazolylethynylene oligomer (Tg-Car) with triethylene glycol monomethyl ether (Tg) side chains was synthesized following steps

reported previously (24). 4-nitrotoluene (NT, 99%) and 2,4-dinitrotoluene (DNT, analytical standard) were purchased from Aldrich. 2,4,6-trinitrotoluene (TNT) was obtained from Dyno Nobel. Other chemicals were purchased from Aldrich or Fisher at the reagent grade and used as received.

2.5.2 Device Fabrication Details

1.0 mg carbon nanotubes and 5.6 mg Tg-Car oligomer were added to 9.0 mL of chloroform and sonicated in a water bath (Fisher Scientific FS30H model) at room temperature for 90 min. Then the suspension was set aside for 30 min. Then suspension was transferred to a centrifugation tube and centrifuged (IEC Centra CL2) at 4200 rpm (~ 3000 g) for 20 min. The supernatant was transferred into another centrifugation tube and the centrifugation process was repeated two more times. The final supernatant is very stable with no precipitate observed after three years.

The IDE were patterned onto a silicon wafer with a 300 nm thermal oxide layer (purchased from Silicon Quest) using a standard photolithography procedure. The gap between fingers in the IDE is 80 μm. The width of the channel is 2100 μm and the length is 20 μm. There are 10 finger pairs in total. The 20 nm adhesive titanium layer and the 50 nm gold layer were sputtered on the wafer.

The IDE chips were cleaned by sonication in acetone, methanol and isopropanol successively. Then the devices were made by drop-casting 2-6 μL (2 μL at a time) of the diluted Tg-Car/CNT suspension (diluted 40 times from the original Tg-Car/CNT suspension, the supernatant after three times of centrifugation above) until the resistances of the sensor devices were within the range of 50 kΩ to 200 kΩ. The devices were heated

at 80 °C for 5 min under ambient environment to remove chloroform residue.

1.0 mg CNTs was placed in 50 mL dimethylformamide (DMF) and sonicated for 2 h. Then the suspension was diluted 50 times. To fabricate the sensor devices, 2-6 μL (2 μL at a time) of the CNT suspension was drop-cast on the pre-cleaned IDE chips until the resistances of the devices were within the range of 50 kΩ to 200 kΩ. Then, the sensor devices were heated at an elevated temperature (~ 120 °C) for 5 min under ambient environment to get rid of extra DMF on the surface of the IDE chips.

Atomic force microscopy (Veeco MultiMode V scanning probe) operating in tapping mode was used to characterize the surface morphology of Tg-Car/CNT film deposited on IDEs. Optical images were obtained using a CCD camera in the microscope.

The sensor devices were wire-bonded into a ceramic chip carrier and connected to an Agilent 4156C Precision Semiconductor Parameter Analyzer. A custom designed Teflon enclosure was used to cover the ceramic chip carrier. A DC voltage (1.0 V) was applied to the electrode and the current was monitored.

2.5.3 Vapor Generation System

Different concentrations of vapor were obtained by mixing the saturated analyte vapor (25) at room temperature with delivery gas (fixed at 100 sccm by a mass flow controller). Either 250 mg of a solid analyte or 0.5 mL of a liquid analyte was placed in a 60 mL glass syringe for 2 h for saturation (Figure 2.3). The saturated analyte vapor at room temperature was infused by the syringe pump (NE-4000 New Era Pump System, Inc.) with different pumping rates. Table 2.1 and Table 2.2 show vapor concentrations diluted from a certain flow rate of saturated vapor. The diluted concentration is calculated from the saturated concentration multiplied by the percentage of the analyte flow rate over the total flow rate.

2.5.4 Calculation of the Limit of Detection

A limit of detection (LOD) of 95 ppb for NT is calculated based on the following equation (26):

$$LOD = 3* rms\_noise/slope \quad (2.1)$$

The slope is 0.0026, which is from the linear fitting the five points in the Figure 2.2b. The noise level (rms_noise) is 0.000082, which is calculated from the root-mean-square deviation of 15 data points from the baseline.

2.6 Acknowledgements

This work was supported by the Department of Homeland Security, Science and Technology Directorate under Grant (2009-ST-108-LR0005), University of Utah and USTAR program. B.R.B. acknowledges funding from the National Science Foundation (DGE0903715), National Aeronautics and Space Administration Office of the Chief Technologist (NNX12AM67H), and the Wayne Brown Fellowship.

2.7 References

(1) Toal, S. J.; Trogler, W. C. Polymer Sensors for Nitroaromatic Explosives Detection. *J. Mater. Chem.* **2006,** *16,* 2871-2883.

(2) Engel, Y.; Elnathan, R.; Pevzner, A.; Davidi, G.; Flaxer, E.; Patolsky, F. Supersensitive Detection of Explosives by Silicon Nanowire Arrays. *Angew. Chem., Int. Ed. Engl.* **2010,** *49,* 6830-6835.

(3) Díaz Aguilar, A.; Forzani, E. S.; Leright, M.; Tsow, F.; Cagan, A.; Iglesias, R. A.; Nagahara, L. A.; Amlani, I.; Tsui, R.; Tao, N. J. A Hybrid Nanosensor for TNT Vapor Detection. *Nano Lett.* **2009,** *10,* 380-384.

(4) Ma, Y.; Wang, S.; Wang, L. Nanomaterials for Luminescence Detection of Nitroaromatic Explosives. *TrAC. Trends Anal. Chem.* **2015,** *65,* 13-21.

(5) Darrach, M. R.; Chutjian, A.; Plett, G. A. Trace Explosives Signatures from World War

II Unexploded Undersea Ordnance. *Environ. Sci. Technol.* **1998,** *32,* 1354-1358.

(6) Perr, J. M.; Furton, K. G.; Almirall, J. R. Solid Phase Microextraction Ion Mobility Spectrometer Interface for Explosive and Taggant Detection. *J. Sep. Sci.* **2005,** *28,* 177-183.

(7) Salinas, Y.; Martinez-Manez, R.; Marcos, M. D.; Sancenon, F.; Costero, A. M.; Parra, M.; Gil, S. Optical Chemosensors and Reagents to Detect Explosives. *Chem. Soc. Rev.* **2012,** *41,* 1261-1296.

(8) Thomas, S. W.; Joly, G. D.; Swager, T. M. Chemical Sensors Based on Amplifying Fluorescent Conjugated Polymers. *Chem. Rev.* **2007,** *107,* 1339-1386.

(9) Bai, M.; Huang, S.; Xu, S.; Hu, G.; Wang, L. Fluorescent Nanosensors via Photoinduced P Polymerization of Hydrophobic Inorganic Quantum Dots for the Sensitive and Selective Detection of Nitroaromatics. *Anal. Chem.* **2015,** *87,* 2383−2388.

(10) Nie, H.; Zhao, Y.; Zhang, M.; Ma, Y.; Baumgarten, M.; Muellen, K. Detection of TNT Explosives with a New Fluorescent Conjugated Polycarbazole Polymer. *Chem. Commun.* **2011,** *47,* 1234-1236.

(11) Kartha, K. K.; Sandeep, A.; Nair, V. C.; Takeuchi, M.; Ajayaghosh, A. A Carbazole-Fluorene Molecular Hybrid for Quantitative Detection of TNT Using a Combined Fluorescence and Quartz Crystal Microbalance Method. *Phys. Chem. Chem. Phys.* **2014,** *16,* 18896-18901.

(12) Zhang, C.; Che, Y.; Yang, X.; Bunes, B. R.; Zang, L. Organic Nanofibrils based on Linear Carbazole Trimer for Explosive Sensing. *Chem. Commun.* **2010,** *46,* 5560-5562.

(13) Che, Y.; Gross, D. E.; Huang, H.; Yang, D.; Yang, X.; Discekici, E.; Xue, Z.; Zhao, H.; Moore, J. S.; Zang, L. Diffusion-Controlled Detection of Trinitrotoluene: Interior Nanoporous Structure and Low Highest Occupied Molecular Orbital Level of Building Blocks Enhance Selectivity and Sensitivity. *J. Am. Chem. Soc.* **2012,** *134,* 4978-4982.

(14) Naddo, T.; Che, Y.; Zhang, W.; Balakrishnan, K.; Yang, X.; Yen, M.; Zhao, J.; Moore, J. S.; Zang, L. Detection of Explosives with a Fluorescent Nanofibril Film. *J. Am. Chem. Soc.* **2007,** *129,* 6978-6979.

(15) Chen, P.-C.; Sukcharoenchoke, S.; Ryu, K.; Gomez de Arco, L.; Badmaev, A.; Wang, C.; Zhou, C. 2,4,6-Trinitrotoluene (TNT) Chemical Sensing Based on Aligned Single-Walled Carbon Nanotubes and ZnO Nanowires. *Adv. Mater.* **2010,** *22,* 1900-1904.

(16) Wang, F.; Gu, H.; Swager, T. M. Carbon Nanotube/Polythiophene Chemiresistive Sensors for Chemical Warfare Agents. *J. Am. Chem. Soc.* **2008,** *130,* 5392-5393.

(17) Robinson, J. T.; Perkins, F. K.; Snow, E. S.; Wei, Z.; Sheehan, P. E. Reduced Graphene Oxide Molecular Sensors. *Nano Lett.* **2008,** *8,* 3137-3140.

(18) Esser, B.; Schnorr, J. M.; Swager, T. M. Selective Detection of Ethylene Gas using Carbon Nanotube-based Devices: Utility in Determination of Fruit Ripeness. *Angew. Chem., Int. Edit.* **2012,** *51,* 5752-5756.

(19) Chen, Y.; Lee, Y. D.; Vedala, H.; Allen, B. L.; Star, A. Exploring the Chemical Sensitivity of a Carbon Nanotube/Green Tea Composite. *ACS Nano* **2010,** *4,* 6854-6862.

(20) Ding, M.; Tang, Y.; Gou, P.; Reber, M. J.; Star, A. Chemical Sensing with Polyaniline Coated Single-Walled Carbon Nanotubes. *Adv. Mater.* **2011,** *23,* 536-540.

(21) Chen, J.; Hamon, M. A.; Hu, H.; Chen, Y.; Rao, A. M.; Eklund, P. C.; Haddon, R. C. Solution Properties of Single-Walled Carbon Nanotubes. *Science* **1998,** *282,* 95-98.

(22) Bunes, B. R.; Xu, M.; Zhang, Y.; Gross, D. E.; Saha, A.; Jacobs, D. L.; Yang, X.; Moore, J. S.; Zang, L. Photodoping and Enhanced Visible Light Absorption in Single-Walled Carbon Nanotubes Functionalized with a Wide Band Gap Oligomer. *Adv. Mater.* **2015,** *27,* 162-167.

(23) Zhang, Z.; Che, Y.; Smaldone, R. A.; Xu, M.; Bunes, B. R.; Moore, J. S.; Zang, L. Reversible Dispersion and Release of Carbon Nanotubes Using Foldable Oligomers. *J. Am. Chem. Soc.* **2010,** *132,* 14113-14117.

(24) Gross, D. E.; Moore, J. S. Arylene–Ethynylene Macrocycles via Depolymerization–Macrocyclization. *Macromolecules* **2011,** *44,* 3685-3687.

(25) Östmark, H.; Wallin, S.; Ang, H. G. Vapor Pressure of Explosives: A Critical Review. Propellants, *Explos*. *Pyrotech.* **2012,** *37,* 12-23.

(26) Li, J.; Lu, Y.; Ye, Q.; Cinke, M.; Han, J.; Meyyappan, M. Carbon Nanotube Sensors for Gas and Organic Vapor Detection. *Nano Lett.* **2003,** *3,* 929-933.

(27) Schnorr, J. M.; van der Zwaag, D.; Walish, J. J.; Weizmann, Y.; Swager, T. M. Sensory Arrays of Covalently Functionalized Single-Walled Carbon Nanotubes for Explosive Detection. *Adv. Funct. Mater.* **2013,** *23,* 5285-5291.

(28) Kong, J.; Franklin, N. R.; Zhou, C.; Chapline, M. G.; Peng, S.; Cho, K.; Dai, H. Nanotube Molecular Wires as Chemical Sensors. *Science* **2000,** *287,* 622-625.

(29) Gao, T.; Woodka, M. D.; Brunschwig, B. S.; Lewis, N. S. Chemiresistors for Array-Based Vapor Sensing Using Composites of Carbon Black with Low Volatility Organic Molecules. *Chem. Mater.* **2006,** *18,* 5193-5202.

(30) García-Berríos, E.; Theriot, J. C.; Woodka, M. D.; Lewis, N. S. Detection of Ammonia, 2,4,6-trinitrotoluene, and Common Organic Vapors using Thin-film Carbon Black-metalloporphyrin Composite Chemiresistors. *Sens. Actuators B Chem.* **2013,** *188,* 761-767.

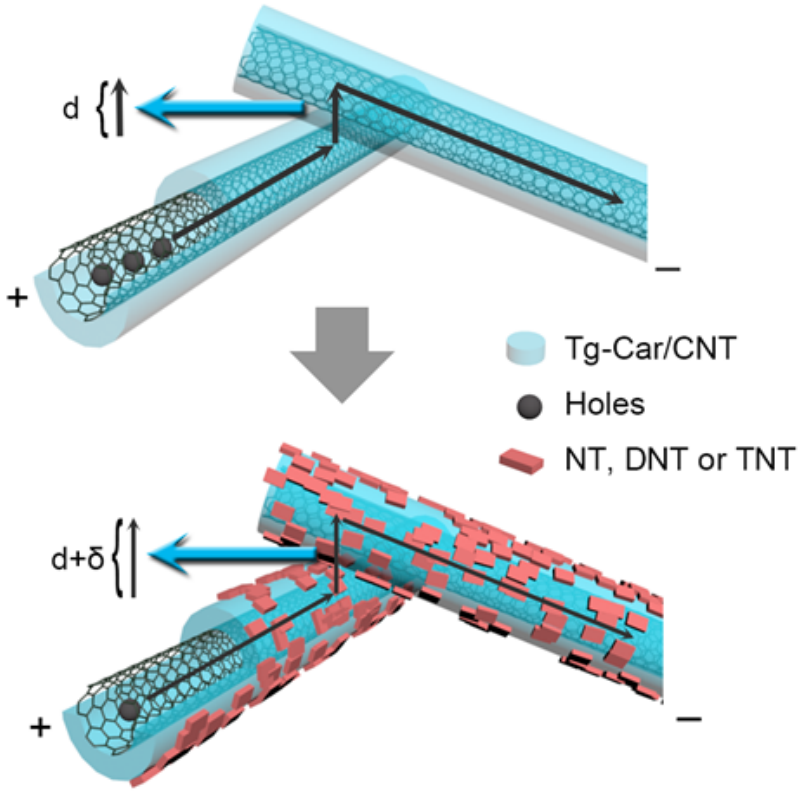

Scheme 2.1 Schematic of the charge carriers (holes) moving in the CNT and tunneling though the Tg-Car oligomer before and after the exposure to NA explosive compounds.

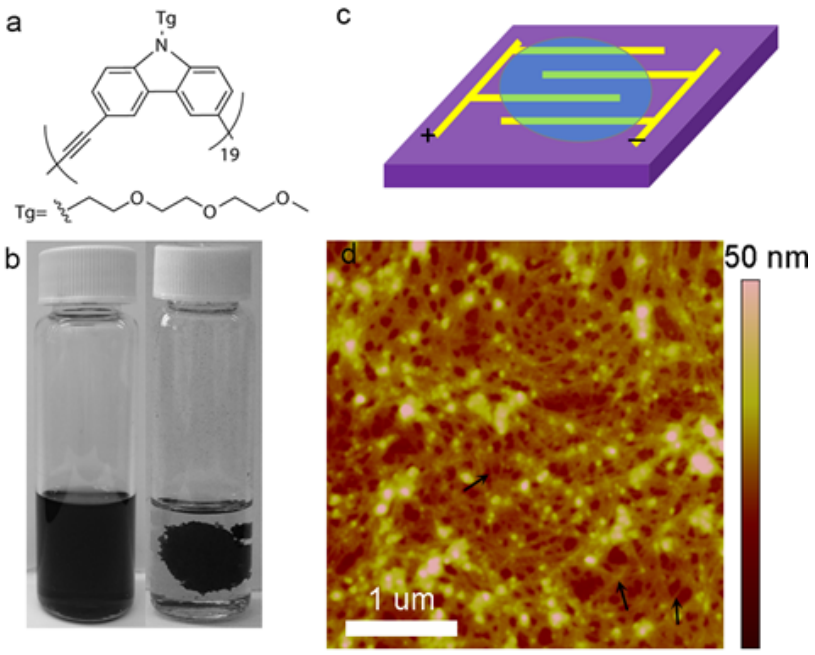

Figure 2.1 (a) Molecular structure of the Tg-Car oligomer. (b) CNT suspensions in chloroform with (left vial) and without Tg-Car oligomer (right vial). (c) Schematic view of the sensor device with the Tg-Car/CNT thin film. (d) AFM image of the Tg-Car/CNT thin film drop-cast on an IDEs chip.

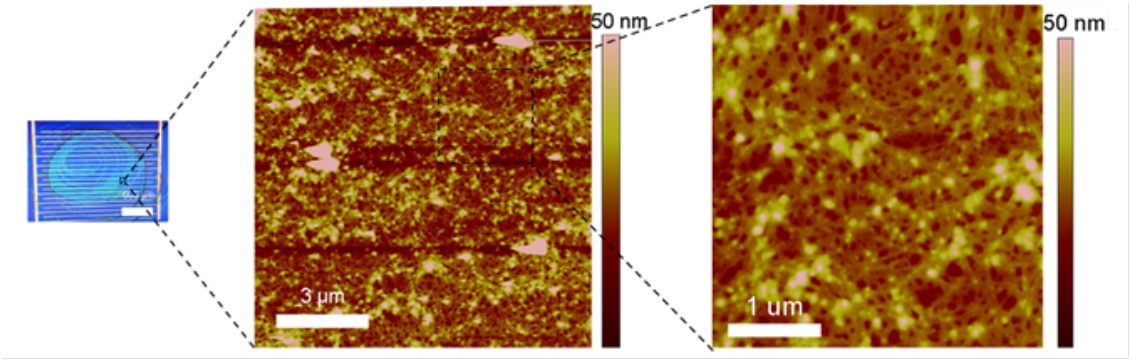

Figure 2.2 Optical microscope image (scale bar: 600 µm) and AFM images of the Tg Car/CNT thin film drop-cast on IDEs.

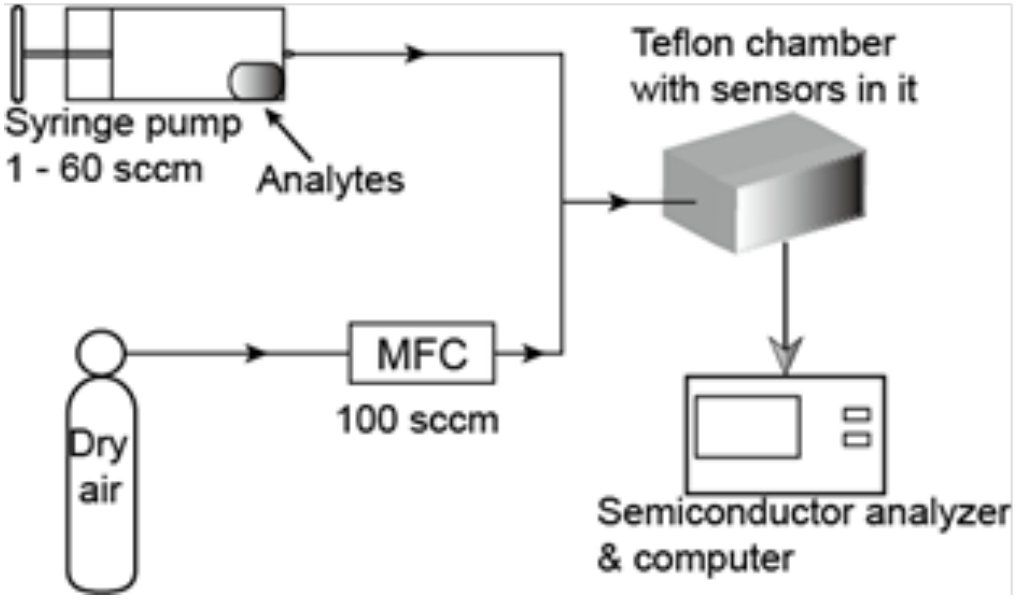

Figure 2.3 Vapor generation and delivery system.

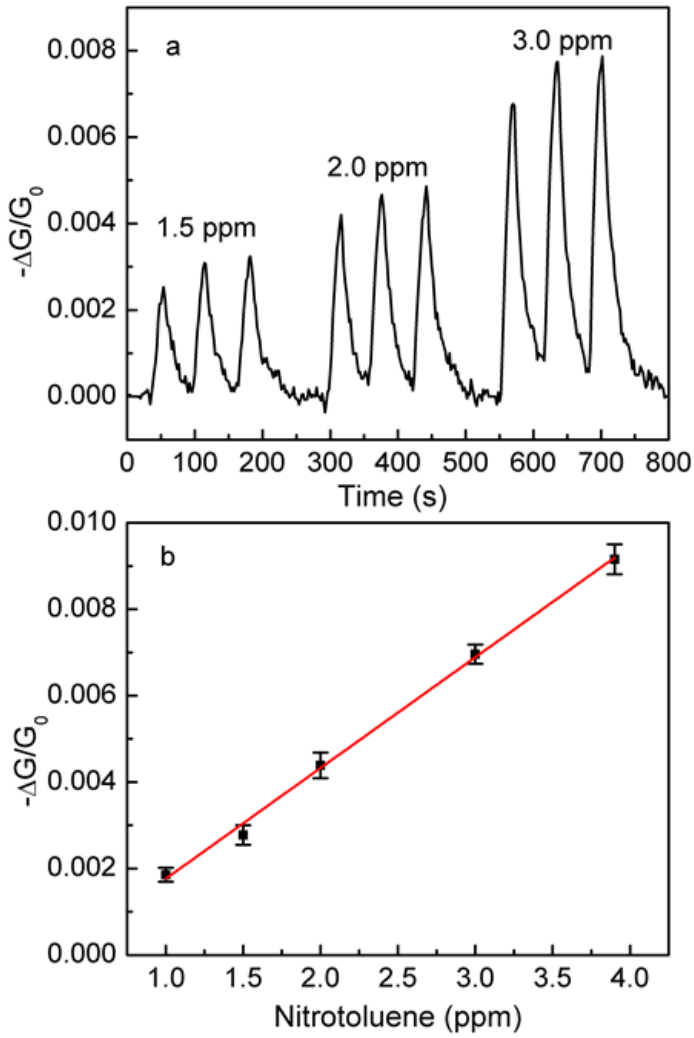

Figure 2.4 (a) Real-time sensory response to NT vapor at concentration of 1.5, 2.0, and 3.0 ppm. The exposure at each concentration was repeated three times. The analyte exposure time is 20 s and the recovery time is 40 s for each test. (b) Calibration curve of the sensor's response at different vapor concentrations of NT, 1.0, 1.5, 2.0, 3.0, and 3.9 ppm.

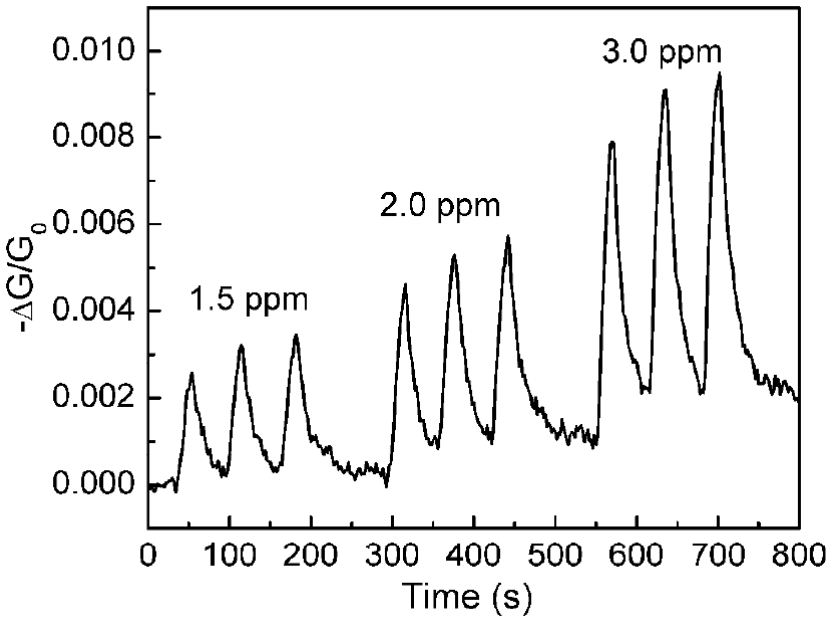

Figure 2.5 The real-time sensory response (without baseline correction, compared to the corrected data presented in Figure 2.2a) to NT at concentration of 1.5 ppm, 2.0 ppm, and 3.0 ppm (Table 2.1). Exposures to each concentration were repeated three times.

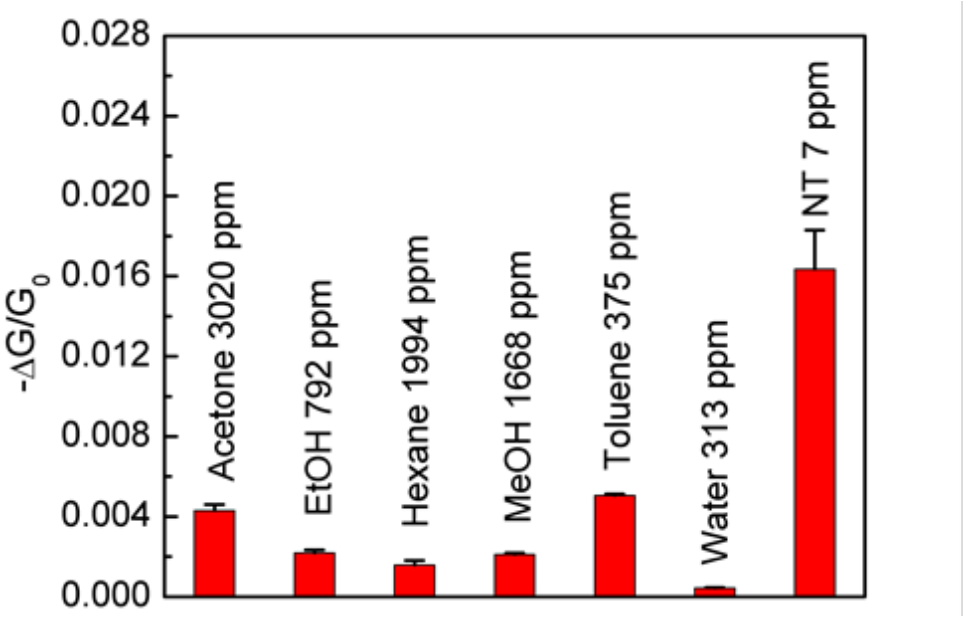

Figure 2.6 Response of the Tg-Car/CNT sensor to NT (15 sccm of saturated vapor diluted with 100 sccm of dry air, about 13% of saturated vapor at room temperature) and other common chemical reagents (1% of saturated vapor at room temperature).

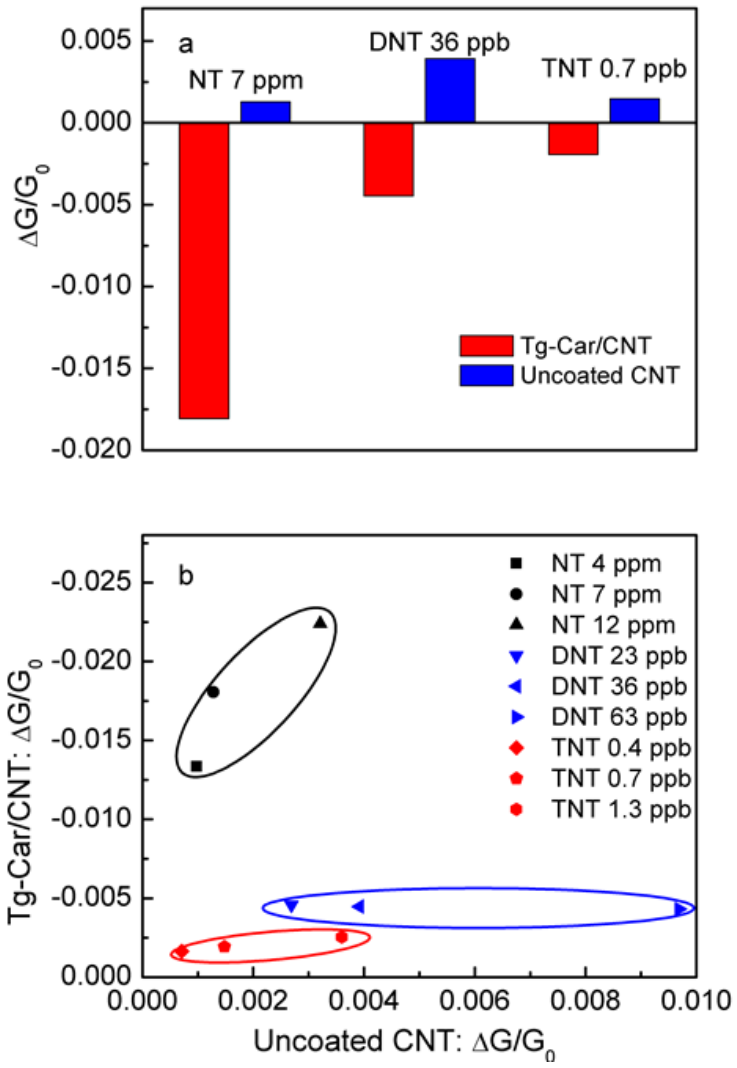

Figure 2.7 (a) Conductance changes of the Tg-Car/CNT sensor and the uncoated CNT sensor in response to NT at 7 ppm, DNT at 36 ppb, and TNT at 0.7 ppb (15 sccm diluted in 100 sccm of dry air). (b) Scatter plot of the conductance changes of the Tg-Car/CNT sensor and uncoated CNT sensor to three different vapor concentrations of NT, DNT and TNT.

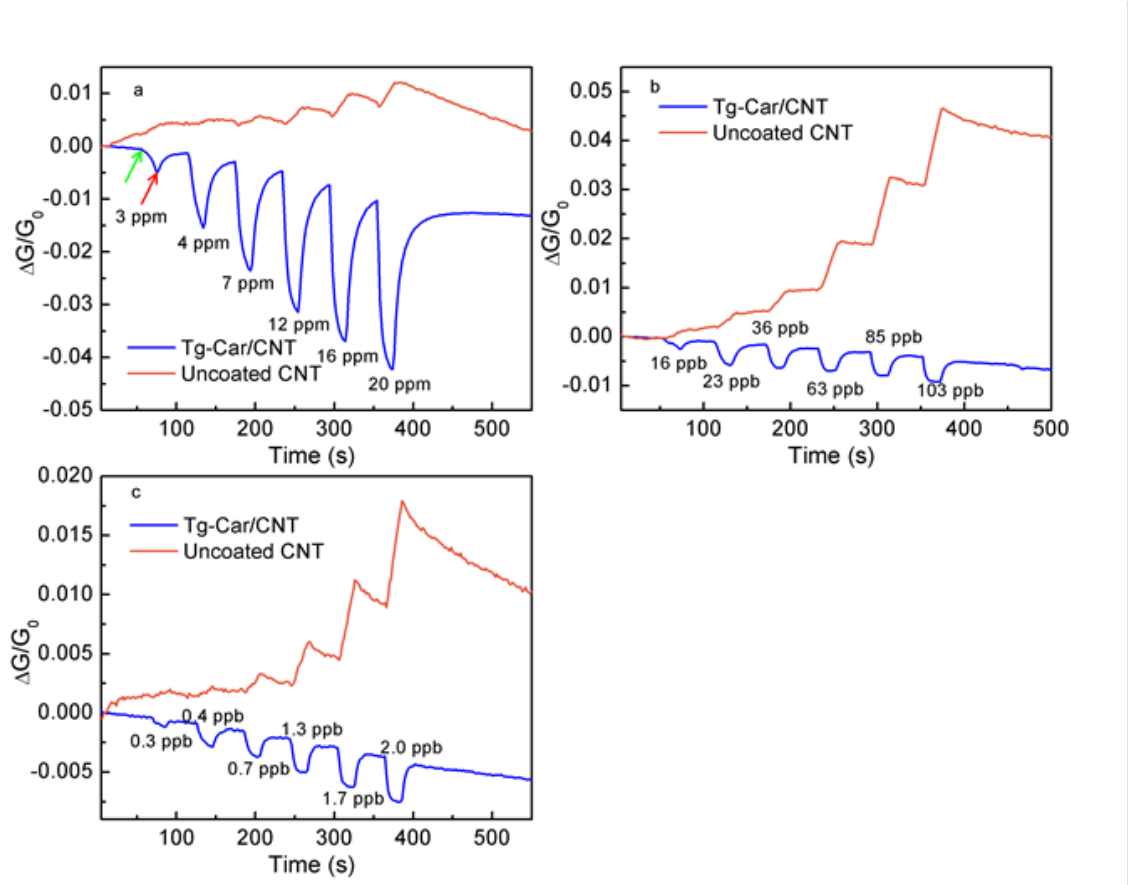

Figure 2.8 The sensory response of the Tg-Car/CNT sensors and the uncoated CNT sensors to (a) NT, (b) DNT and (c) TNT vapor at different concentrations diluted from 6 sccm, 9 sccm, 15 sccm, 30 sccm, 45 sccm, and 60 sccm of corresponding saturated vapor at room temperature. The green arrow represents the beginning of the exposure to an analyte and the red arrow represents the end of the exposure to an analyte. The time for the exposure to an analyte is 20 s and the recovery time is 40 s for each test.

Table 2.1 Vapor concentrations and flow rates for Figure 2.4 and Figure 2.5.

	Vapor Pressure 23 °C (Torr)	**Estimated Concentration**	**Analyte flow rate: 2 sccm**	**3 sccm**	**4 sccm**	**6 sccm**	**8 sccm**
NT	4.02e-2	52.9 ppm	1.0 ppm	1.5 ppm	2.0 ppm	3.0 ppm	3.9 ppm

Table 2.2 Vapor concentrations for Figure 2.7.

	Vapor Pressure 23 °C (Torr)	Estimated Concentration	Analyte flow rate: 9 sccm	Analyte flow rate: 15 sccm	Analyte flow rate: 30 sccm
NT	4.02e-2	52.9 ppm	4 ppm	7 ppm	12 ppm
DNT	2.08e-4	274 ppb	23 ppb	36 ppb	63 ppb
TNT	4.12e-6	5.42 ppb	0.4 ppb	0.7 ppb	1.3 ppb

CHAPTER 3

POLY(3-ALKYLTHIOPHENE)/CNT-BASED CHEMIRESISTIVE SENSORS FOR VAPOR DETECTION OF LINEAR ALKANES: EFFECT OF POLYMER SIDE CHAIN LENGTH[1]

3.1 Abstract

In general, alkane vapors are difficult to detect due to their nonreactive nature at room temperature. Here, we show chemiresistive sensors made of carbon nanotubes (CNTs) noncovalently functionalized with three kinds of poly(3-alkylthiophene) (P3AT), namely, poly(3-butylthiophene) (P3BT), poly(3-octylthiophene-2,5-diyl) (P3OT) and poly(3-dodecylthiophene-2,5-diyl) (P3DT). We compared the responses of sensors composed of these materials to four linear alkanes, hexane, octane, decane, and dodecane. The results show that sensors with CNTs functionalized with P3ATs that have alkyl side chains with length similar to the length of the analyte alkane produced a bigger response than the case in which the lengths are different. Based on this response trend, a sensor array was made, which can distinguish different sizes of linear alkane vapors. This work facilitates the future design of CNT-based sensor arrays for distinguishing analytes with similar physical

---

[1]Adapted by permission from Zhang, Y.; Bunes, B. R.; Wang, C.; Wu, N.; Zang, L. Poly(3-alkylthiophene)/CNT-based Chemiresistive Sensors for Vapor Detection of Linear Alkanes: Effect of Polymer Side Chain Length. *Sens Actuators B Chem.* **2017,** 247, 713-717.

and chemical properties.

3.2 Introduction

Alkanes are hydrocarbons with only single carbon-carbon bonds and no functional groups, yet alkanes are important to human beings. They are commonly used as fuels and are also widely used in industry. However, they have safety issues including explosion (1) and inhalational toxicity (2). The Occupational Safety and Health Administration (OSHA) in the United States has regulated the permissible exposure limit of n-hexane to be 500 ppm (3). Thus, a portable, low-cost, and reliable vapor sensor for detecting and distinguishing alkanes would benefit us in aspects such as detecting fuel leaks in airplanes, detecting homemade explosives made of nitrate-fuel oil mixtures, and monitoring the environmental exposure of alkanes. However, it is difficult to make highly sensitive alkane sensors due to their lack of reactivity at room temperature and they have similar chemical and physical properties. Previous research has been done using traditional instruments, such as Fourier transform infrared (FTIR) spectrometry (4), gas chromatography (5) and ion mobility spectrometry (6). However, those methods involve expensive and bulky instruments and the testing processes are time-consuming. Emerging methods have been developed using nanomaterials such as metal oxide thin films (7), gold nanoparticles (8-9), silicon nanowires (10), and organic nanofibers (11). However, those sensors usually have specific operational requirements such as high operation temperatures, sophisticated measurement equipment, or light irradiation. Those requirements hinder the development of those sensors.

Chemiresistive sensors based on carbon nanotubes (CNTs) have attracted significant attention due to their high sensitivity (12-13), simple fabrication process (14), and simple

operational requirements. To further enhance their sensitivity and selectivity, covalent (15-16) and noncovalent (17-18) functionalizations were introduced to CNT-based chemiresistive sensors. Most of these functionalized sensors work through an interaction between the sensor and the analyte such as hydrogen bonding (15), halogen bonding (19), electrostatic effect (20), and the creation of a chemical reaction (21). However, none of those methods work in an alkane sensor because of the lack of a specific chemical functional group and the unreactive nature of alkanes at room temperature.

Here, we demonstrate chemiresistive alkane sensors based on CNTs coated with poly(3-alkylthiophene) (P3AT). P3ATs with different side alkyl chain lengths were used in this study, namely, poly(3-butylthiophene-2,5-diyl) (P3BT), poly(3-octylthiophene-2,5-diyl) (P3OT), poly(3-dodecylthiophene-2,5-diyl) (P3DT) (Scheme 3.2a). We have tested the responses of these P3ATs/CNT sensors to four linear alkanes, namely, n-hexane, n-octane, n-decane and n-dodecane (Scheme 3.2b). There are three features in our design. (1) P3ATs greatly enhance the dispersion of CNTs in solvents, which makes the fabrication process simple and repeatable. Meanwhile, good dispersion of CNT facilitates the fabrication of a continuous, uniform percolation network of CNTs, which is conducive to gas diffusion and adsorption, thereby facilitating application in vapor sensing. (2) Polythiophenes with a variety of types of side chains are commercially available so we can easily replace the polymer with different side chain lengths and other functional groups to further improve the detection selectivity. (3) The sensors are most responsive to the alkane with similar chain length as the side-chain of P3AT, a mechanism based on the general chemistry principle “like dissolves like.” This trend of response could be used to distinguish the size of alkane molecules in a vapor. This research is a proof of concept of designing a sensor array with polymer functionalized CNTs, which can potentially

distinguish similar analytes.

3.3 Materials and Methods

3.3.1 P3AT/CNT Preparation Method

The P3AT/CNT suspensions used for making the sensors were prepared through the following steps. First, CNTs were suspended in 1,2-dichlorobenzene (ODCB) with a concentration of 1 mg/mL, followed by 2 h of sonication in a sonication bath. P3ATs were dissolved in ODCB with a concentration of 5 mg/mL. Second, the two solutions were mixed to achieve the CNT suspension, in which the weight ratio of P3AT: CNT was 3:1. The mixtures were sonicated for 2 h in a sonication bath. Subsequently, about 10 vol% of cyclohexanone was quickly injected into the mixture to facilitate the aggregation of P3ATs onto CNTs (22). The mixtures were then kept undisturbed overnight to reach equilibrium. The mixtures thus obtained were relatively homogeneous and dark black. Since the precipitates were not removed, agitation was needed to make the suspension uniform. Third, the mixtures were agitated for several seconds and diluted in ODCB to achieve a concentration of CNTs of 2.5 μg/mL (estimated) and the diluted suspensions were sonicated for 2 h. Then, the diluted suspensions were ready to use. The diluted suspensions were stable with no aggregates formed over 6 months on a benchtop at room temperature, with the exception of the P3BT/CNT suspension, which formed aggregates after a few weeks (see the photos in Figure 3.1). After sonicating for several minutes, the aggregation in the diluted suspension of P3BT/CNT would disappear and the suspension would be ready to use again. These uniform and stable P3AT/CNT suspensions make the fabrication process facile and reproducible.

3.3.2 Sensor Device Preparation Method

Sensors were fabricated by drop-casting one of the diluted P3AT/CNT suspensions onto pre-patterned interdigitated electrodes (IDEs) followed by heating at 120 °C for 10 min in an ambient environment to remove the remaining solvent. After the solvent evaporated, the electrical resistance of the IDE was tested. The drop-casting of the suspension was continued until the resistance of the device reached 20 – 200 kΩ, forming a thin film of P3AT/CNT on the IDEs. Scanning electron microscopy (Figure 3.2) shows the porous and continuous structure of a P3OT/CNT thin film, which is beneficial for a vapor sensor because analyte molecules can penetrate into this thin film.

3.4 Results and Discussion

3.4.1 Characterizations

UV-Vis absorption spectra were obtained from the three P3AT/CNT suspensions (Figure 3.1). There were additional peaks around 610 nm in the P3AT/CNT suspensions, indicating the formation of a highly ordered structure of P3ATs due to their aggregation on the surface of CNTs (23-24). The overall baseline of the P3AT/CNT absorption spectra increased when the alkyl side chain length increases. This indicates that P3ATs with longer alkyl side chain have stronger abilities to disperse CNTs in solvent. Atomic force microscopy (AFM) was used to characterize the dispersion of CNTs. The AFM image (Figure 3.1d) indicates that CNTs were individually dispersed. The height distribution study in Figure 3.3 shows that the average diameter of the CNTs in the P3OT/CNT suspension is around 1.1 ± 0.2 nm. Comparing with the manufacture's data and our previous study (25), this is an almost 40% increase of diameter from bare CNTs (0.8 ± 0.1 nm). This demonstrates the addition of the P3OT coating on the surface of CNTs. All those

characterizations demonstrate the uniform coating of P3ATs on the surface of the CNTs, as well as the individual dispersion of CNTs thus produced.

3.4.2 Sensitivity and Limit of Detection to n-Dodecane

The sensitivity of those sensors to alkane is first presented with n-dodecane using a P3DT/CNT sensor. Figure 3.4a shows the three times repeated testing of a P3DT/CNT device by exposing to 1%, 2%, 4%, and 8% dilution of saturated vapor of n-dodecane (Table 3.1 shows the saturated vapor pressures of the four alkane analytes at 20 °C). Overall, the sensor's response to n-dodecane is fast, recoverable, and reproducible. Figure 3.4b shows that the sensor displays a linear response to n-dodecane from 1% to 8%. A limit of detection (LOD) of 342 ppb was projected for n-dodecane following the linear fitting, and similarly a LOD of 76 ppm was projected for n-hexane (see section 3.6.4 of this dissertation for more detail). The LOD of 76 ppm of n-hexane is far lower than OSHA's permissible exposure limit of 500 ppm, demonstrating the utility of the sensor.

3.4.3 The Effect of Side Chain Length and the Sensor Array

Then, the responses of all three P3AT/CNT sensors to all four alkanes were measured. Figure 3.5 shows the baseline corrected testing results. When exposed to n-hexane (Figure 3.5a), the P3BT/CNT sensor gave the biggest response, which is about 45% larger than the response of P3DT/CNT. However, the P3DT/CNT sensor gave the biggest response to n-dodecane (Figure 3.5b), which is about 80% larger than the response of P3BT/CNT. Figure 3.5c shows the summary of the sensors' response to all the four alkane analytes. As indicated from the first arrow in Figure 3.5c, the sensor response to n-hexane decreased as the length of the side chain in the P3AT decreased. On the contrary, the sensor response to

n-dodecane increased as the length of the side chain in the P3AT increased. The responses of three kinds of P3AT/CNT sensors to water vapor were tested as well to evaluate the usage in more complex real-life situations (Figure 3.6). All the sensors show much smaller response to water vapor (2504 ppm, 8% of saturated vapor) even compared with much lower vapor of dodecane (14 ppm, 8% of saturated vapor).

The different trends of response observed for the three sensors towards the alkanes vapor as shown in Figure 3.5d demonstrates the capability of distinguishing the different sizes of alkanes by incorporating the three sensors into an array. Figure 3.5d is the principle component score plot of the sensor array. It is clearly seen that the small alkane like n-hexane can be distinguished from the large ones due to the different dissolution preference into the interdigitated polymer side-chain junctions between CNTs. As the size (carbon chain length) of alkanes increases, the dependence of dissolution on the polymer chains becomes less distinct, and consequently it becomes more difficult to discriminate among the long alkanes as shown in Figure 3.5d.

3.4.4 The Sensing Mechanism

The mechanism of the sensor is likely due to the swelling of P3ATs on the surface of CNTs. (11, 26) CNTs form a conductive network, while P3ATs act as the insulating layer between each junction of CNTs in the network. Because the electrode gap is much longer than the CNTs, a charge must cross many of these junctions to get from one electrode to the other. When the sensors are exposed to alkane vapor, P3ATs on the surface absorb it and swell, causing spatial enlargement of the CNT junctions. As a result, the resistance of the CNT network increased and measured as a decrease in current. The porous structure of the CNT network thin film is easily penetrable by the vapor molecules, and the large

interfacial area between adjacent CNTs in the network facilitates the sensor response. Selectivity between alkanes can be understood in two ways. First, shorter alkyl chains of P3AT are less able to accommodate longer alkanes because of their small size; hence, n-hexane elicits a larger response from P3BT/CNT than P3DT/CNT. Conversely, larger alkyl chains of P3AT can accommodate both small and large alkanes, but larger alkanes cause a greater disruption to the interface (i.e., they cause more extensive swelling of the polymer side chains), thus leading to more pronounced sensor response.

3.5 Conclusions

We utilized P3ATs with three side chain lengths to detect four kinds of alkane vapors at low concentrations. The sensing results indicate that the P3AT/CNT sensors with longer side chain lengths, such as P3DT, show bigger responses to longer carbon chain analytes such as n-dodecane. On the contrary, the P3AT/CNT sensors with shorter side chain lengths, such as P3BT, show bigger responses to analytes with shorter carbon chains, such as n-hexane. Thus, by comparing the relative responses of the P3BT/CNT sensors and the P3DT/CNT sensors, we were able to selectively detect those alkane analytes within a certain range of vapor concentrations. The sensors were prepared by simply drop-casting P3AT/CNT suspensions onto IDEs. The mechanism of the response is likely due to the swelling of the P3ATs insulting layers in the conductive CNT network. Future work may involve expanding the polythiophene/CNT sensor array with other side chain functional groups, and the sensor array's ability to differentiate a wide variety of analytes and interruptive vapors would be tested.

3.6 Experimental Methods and Materials

3.6.1 Materials and Interdigitated Electrodes

Carbon nanotubes (SG65i, single walled, >95% semiconducting species) were purchased from SouthWest NanoTechnologies. P3ATs, regioregular, were purchased from Rieke Metals. Alkanes were purchased from TCI. All the other chemicals were purchased from Sigma Aldrich or Fisher and used as received.

The interdigitated electrodes (IDE) were patterned onto a silicon wafer covered with a 300 nm thermal oxide layer (purchased from Silicon Quest) using a standard photolithography procedure. The gap between fingers in the IDE is 80 μm. The width of the channel is 2100 μm and the length is 20 μm. There are 10 finger pairs in total. The IDE fingers consisted of 20 nm adhesive titanium layer and a 50 nm gold layer, which were sputtered on the wafer using a Denton Discovery 18 sputter coater. The IDEs were cleaned by sonicating in acetone, methanol, and isopropanol successively and dried with a nitrogen spray gun and heat at 80 °C for 5 min.

3.6.2 Characterization Methods

Atomic force microscopy (AFM) imaging was performed with a Veeco MultiMode V scanning probe microscopy in a tapping mode, which is suited for characterizing the dispersion of CNTs. The sample for AFM imaging (Figure 3.1d) was prepared by dropping 2 μL of the diluted P3OT/CNT suspension on to a cleaned silicon dioxide surface for several seconds and the suspension on the surface was removed using Kimwipes at the edge of the chip. UV-Vis absorption spectra were measured on an Agilent Cary 100 UV-Vis spectrophotometer. SEM images of the P3OT/CNT thin film were acquired using a Quanta 600 electronic microscope at high vacuum. The preparation procedures of the SEM

samples are the same as the one used in making the sensors (described in the section 3.3 of this dissertation).

3.6.3 Sensor Testing System

The analyte vapor generation and testing system was described in our previous study (14). Briefly, saturated vapor of an alkane analyte at room temperature was pulled from the glass bottle (one gallon) with about 50 mL of liquid alkane analyte on the bottom. A programmed syringe pump (NE-4000 New Era Pump System, Inc.) was used to inject the saturated alkane vapor into a flow of dry air (as carrier gas). The syringe pump was programed to infuse 20 s of the saturated analyte vapor at a certain rate to the carrier gas with a duty cycle of 60 s in order to achieve different diluted vapor concentrations of alkane analyte. The process was repeated three times to examine the reproducibility of sensor response. The diluted vapor was delivered to a PTFE chamber with sensors inside. The sensors were wire-bonded to a ceramic chip carrier and connected to an Agilent 4156C Precision Semiconductor Parameter Analyzer. The sensors were operated at a constant DC bias of 1.0 V and the electrical currents were monitored by the semiconductor analyzer. Matlab and Microsoft Excel were used to perform the baseline correction and the data analysis.

3.6.4 Calculation of the Limit of Detection

A limit of detection (LOD) of 342 ppb for n-dodecane was calculated based on the linear fitting in Figure 3.4b, following the equation: LOD (ppm) = 3* rms_noise/slope * saturated_concentration (ppm) (13). The slope obtained from Figure 3.4b is 0.0596. The noise level (rms_noise) is 0.003996, which is calculated from the root-mean-square

deviation of 15 data points from the baseline.

A limit of detection (LOD) of 76 ppm for n-hexane was calculated based on the linear fitting in Figure 3.7. The slope obtained from Figure 3.7 is 0.1824. The noise level (rms_noise) is 0.00267.

3.7 Acknowledgements

This work was supported by the Department of Homeland Security, Science and Technology Directorate under Grant (2009-ST-108-LR0005), the National Science Foundation under Grant (IIP-1059286) to the American Society for Engineering Education and USTAR program.

3.8 References

(1) R.K. Eckhoff, Explosion Hazards in the Process Industries, 2nd ed., GulfProfessional Publishing, Amsterdam, 2016.

(2) W.E. Luttrell, W.W. Jederberg, K.R. Still, Toxicology Principles for the IndustrialHygienist, American Industrial Hygiene Association, Fairfax, VA, 2008.

(3) Occupational Health Guideline for Hexane, U.S. Department of Health andHuman Services; U.S. Department of Labor, Washington, DC, 1978.

(4) T.G. Levitskaia, J.M. Peterson, E.L. Campbell, A.J. Casella, D.R. Peterman, S.A.Bryan, Fourier transform infrared spectroscopy and multivariate analysis foronline monitoring of dibutyl phosphate degradation product in tributylphosphate/n-dodecane/nitric acid solvent, Ind. Eng. Chem. Res. 52 (2013)17607–17617.

(5) B. Grabowska-Polanowska, J. Faber, M. Skowron, P. Miarka, A. Pietrzycka, I.´Sliwka, A. Amann, Detection of potential chronic kidney disease markers inbreath using gas chromatography with mass-spectral detection coupled withthermal desorption method, J. Chromatogr. A 1301 (2013) 179–189.

(6) S.M., N.J. Vasa, V. Agarwal, J. Chandapillai, UV photo-ionization basedasymmetric field differential ion mobility sensor for trace gas detection, Sens. Actuators B: Chem. 195 (2014) 44–51.

(7) M.C. Carotta, V. Guidi, G. Martinelli, M. Nagliati, D. Puzzovio, D. Vecchi,Sensing of volatile alkanes by metal-oxide semiconductors, Sens. Actuators B:Chem. 130 (2008) 497–501.

(8) E. García-Berríos, T. Gao, M.D. Woodka, S. Maldonado, B.S. Brunschwig, M.W.Ellsworth, N.S. Lewis, Response versus chain length of alkanethiol-capped Aunanoparticle chemiresistive chemical vapor sensors, J. Phys. Chem. C 114(2010) 21914–21920.

(9) H. AlQahtani, M. Sugden, D. Puzzovio, L. Hague, N. Mullin, T. Richardson, M.Grell, Highly sensitive alkane odour sensors based on functionalised goldnanoparticles, Sens. Actuators B: Chem. 160 (2011) 399–404.

(10) B. Wang, H. Haick, Effect of chain length on the sensing of volatile organiccompounds by means of silicon nanowires, ACS Appl. Mater. Interfaces 5(2013) 5748–5756.

(11) C. Wang, B.R. Bunes, M. Xu, N. Wu, X. Yang, D.E. Gross, L. Zang, Interfacialdonor–acceptor nanofibril composites for selective alkane vapor detection, ACS Sens. 1 (2016) 552–559.

(12) D.R. Kauffman, A. Star, Carbon nanotube gas and vapor sensors, Angew. Chem.Int. Ed. 47 (2008) 6550–6570.

(13) J. Li, Y. Lu, Q. Ye, M. Cinke, J. Han, M. Meyyappan, Carbon nanotube sensors forgas and organic vapor detection, Nano Lett. 3 (2003) 929–933.

(14) Y. Zhang, M. Xu, B.R. Bunes, N. Wu, D.E. Gross, J.S. Moore, L. Zang,Oligomer-coated carbon nanotube chemiresistive sensors for selectivedetection of nitroaromatic explosives, ACS Appl. Mater. Interfaces 7 (2015)7471–7475.

(15) F. Wang, T.M. Swager, Diverse chemiresistors based upon covalently modifiedmultiwalled carbon nanotubes, J. Am. Chem. Soc. 133 (2011) 11181–11193.

(16) M. Ding, D.C. Sorescu, A. Star, Photoinduced charge transfer and acetonesensitivity of single-walled carbon nanotube-titanium dioxide hybrids, J. Am.Chem. Soc. 135 (2013) 9015–9022.

(17) Y.-L. Zhao, J.F. Stoddart, Noncovalent functionalization of single-walledcarbon nanotubes, Acc. Chem. Res. 42 (2009) 1161–1171.

(18) N.J. Kybert, M.B. Lerner, J.S. Yodh, G. Preti, A.T.C. Johnson, Differentiation ofcomplex vapor mixtures using versatile DNA–carbon nanotube chemicalsensor arrays, ACS Nano 7 (No. 3) (2013) 2800–2807.

(19) J.G. Weis, J.B. Ravnsbæk, K.A. Mirica, T.M. Swager, Employing halogen bondinginteractions in chemiresistive gas sensors, ACS Sens. 1 (2016) 115–119.

(20) L. Wei, D. Lu, J. Wang, H. Wei, J. Zhao, H. Geng, Y. Zhang, Highly sensitivedetection of trinitrotoluene in water by chemiresistive sensor based onnoncovalently amino functionalized single-walled carbon nanotube, Sens.Actuators B: Chem. 190 (2014) 529–534.

(21) S. Ishihara, J.M. Azzarelli, M. Krikorian, T.M. Swager, Ultratrace detection oftoxic chemicals: triggered disassembly of supramolecular nanotubewrappers, J. Am. Chem. Soc. 138 (2016) 8221–8227.

(22) S. Ren, M. Bernardi, R.R. Lunt, V. Bulovic, J.C. Grossman, S. Gradeˇcak, Towardefficient carbon nanotube/P3HT solar cells: active layer morphology, electrical, and optical properties, Nano Lett. 11 (2011) 5316–5321.

(23) H. Gu, T.M. Swager, Fabrication of free-standing, conductive, and transparentcarbon nanotube films, Adv. Mater. 20 (2008) 4433–4437.

(24) T. Schuettfort, H.J. Snaith, A. Nish, R.J. Nicholas, Synthesis and spectroscopiccharacterization of solution processable highly ordered polythiophene–carbon nanotube nanohybrid structures, Nanotechnology 21(2010) 025201.

(25) B.R. Bunes, M. Xu, Y. Zhang, D.E. Gross, A. Saha, D.L. Jacobs, X. Yang, J.S. Moore,L. Zang, Photodoping and enhanced visible light absorption in single-walled carbon nanotubes functionalized with a wide band gap oligomer, Adv. Mater.27 (2015) 162–167.

(26) E.J. Severin, B.J. Doleman, N.S. Lewis, An investigation of the concentrationdependence and response to analyte mixtures of carbon black/insulatingorganic polymer composite vapor detectors, Anal. Chem. 72 (2000) 658–668.

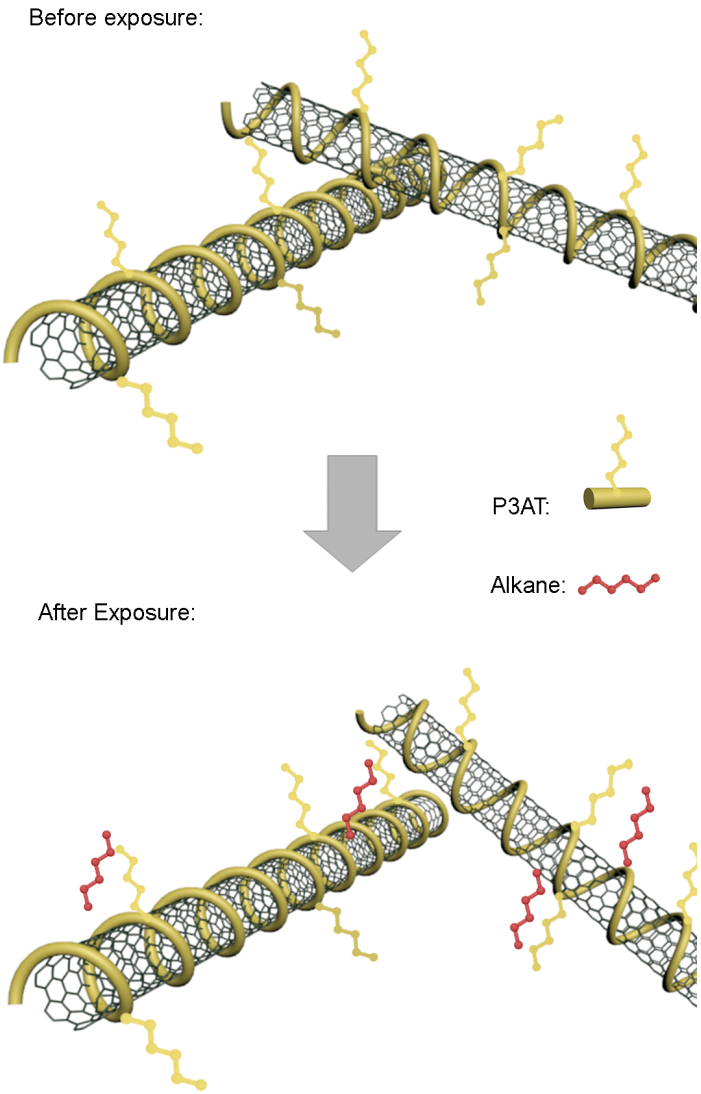

Scheme 3.1 Schematic of the mechanism of the P3AT/CNT sensor.

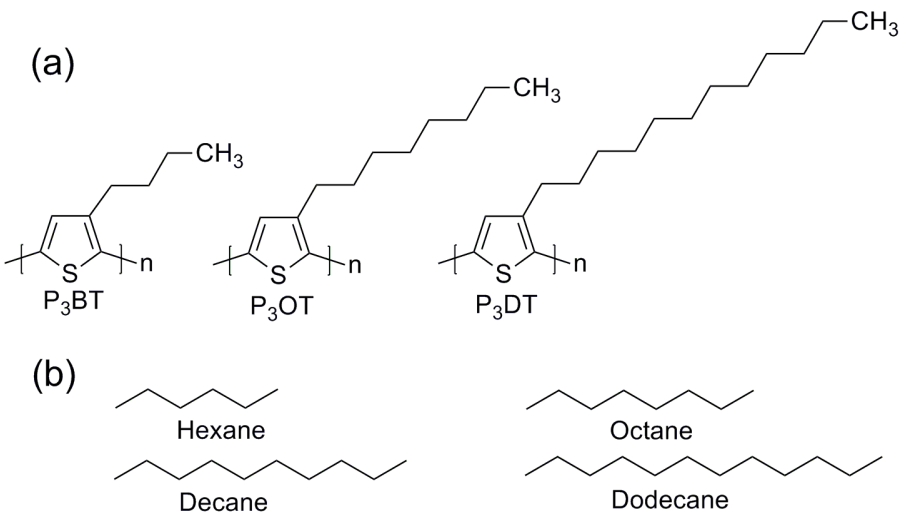

Scheme 3.2 Molecular structure of the three P3ATs (a) and four linear alkane analytes. (b) used in this study.

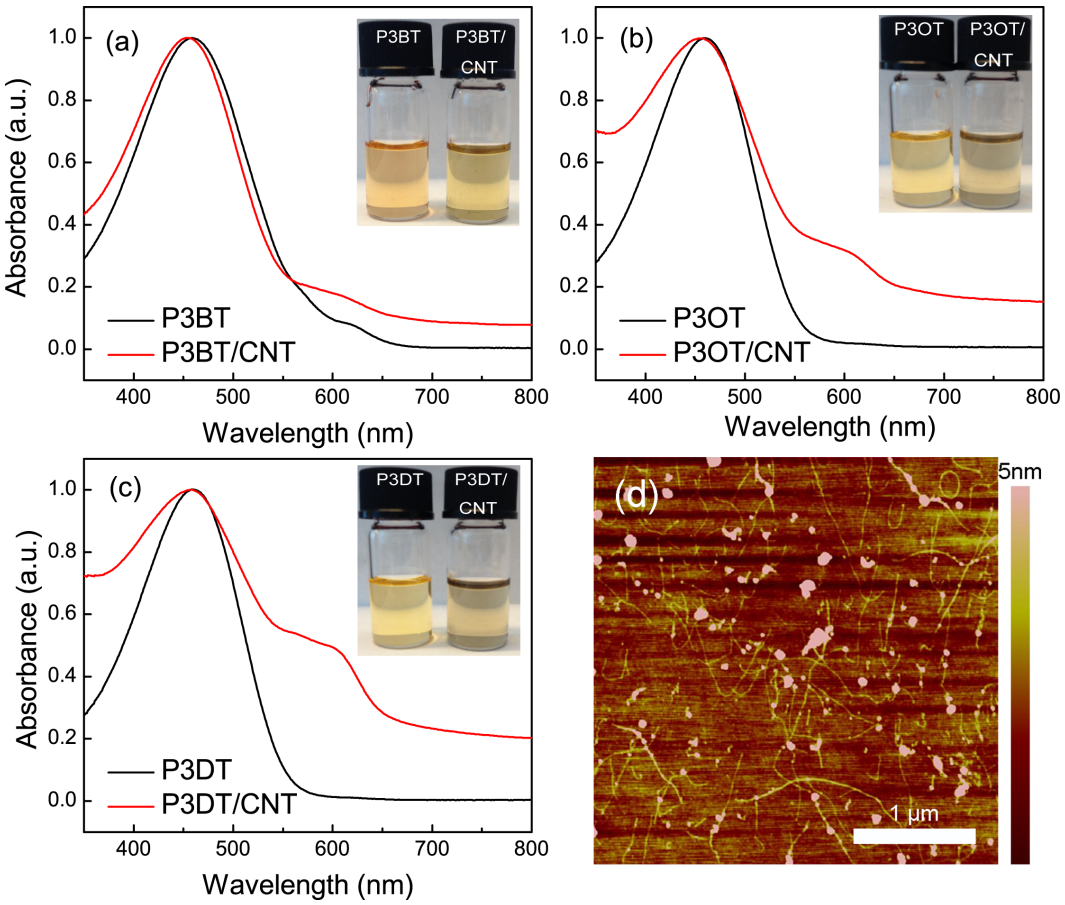

Figure 3.1 (a-c) The UV-Vis absorption spectra and photos of P3AT solutions (0.0075 mg/mL) and P3AT/CNT suspensions. (d) AFM image of the P3OT/CNT suspension cast on a silicon dioxide surface.

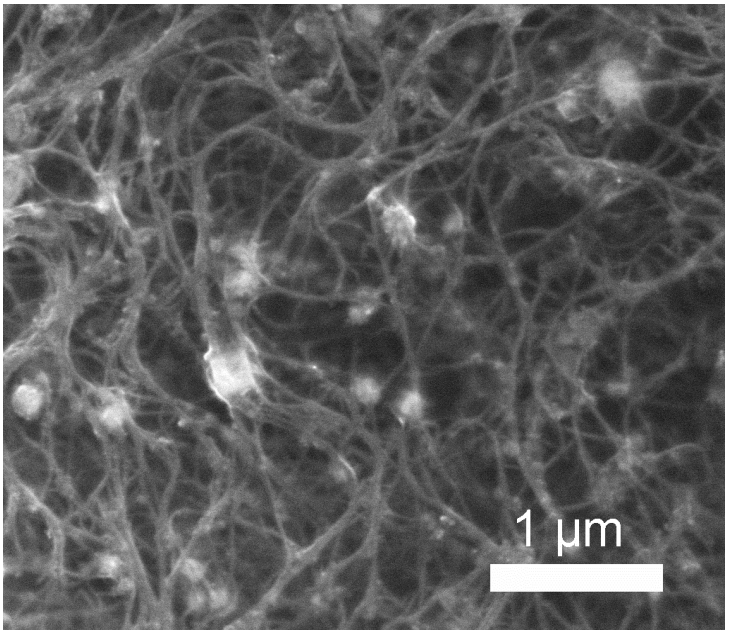

Figure 3.2 SEM image of a P3OT/CNT thin film.

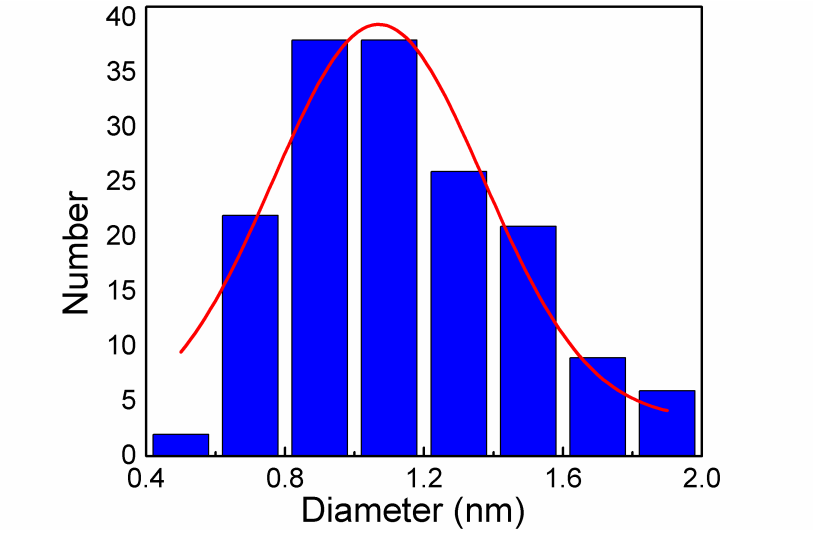

Figure 3.3 Histogram of CNT diameters (blue) extracted from the AFM image in Figure 3.1d and Gaussian fitting of the histogram (red).

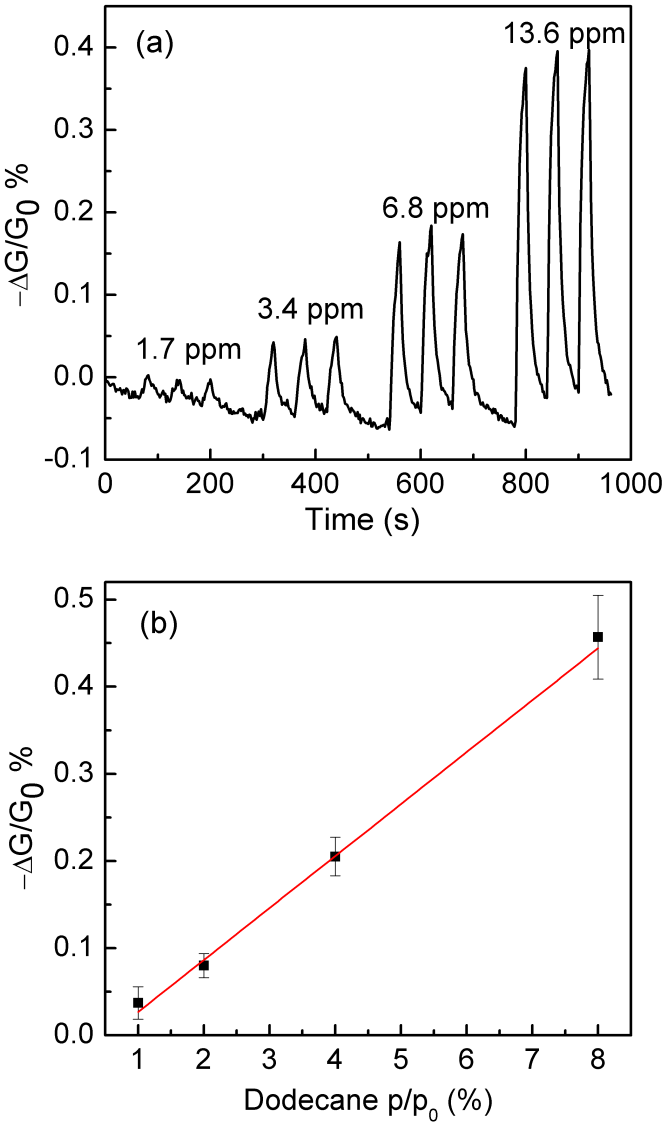

Figure 3.4 (a) Real-time sensor responses to 1% (1.7 ppm), 2% (3.4 ppm), 4% (6.8 ppm) and 8% (13.6 ppm) dilution of the saturated vapor of n-dodecane measured from a P3DT/CNT sensor. The analyte exposure time is 20 s and the recovery time is 40 s. (b) the linear fitting of the sensor's responses to the vapor concentration of n-dodecane; data points were averaged from three independent sensors' responses.

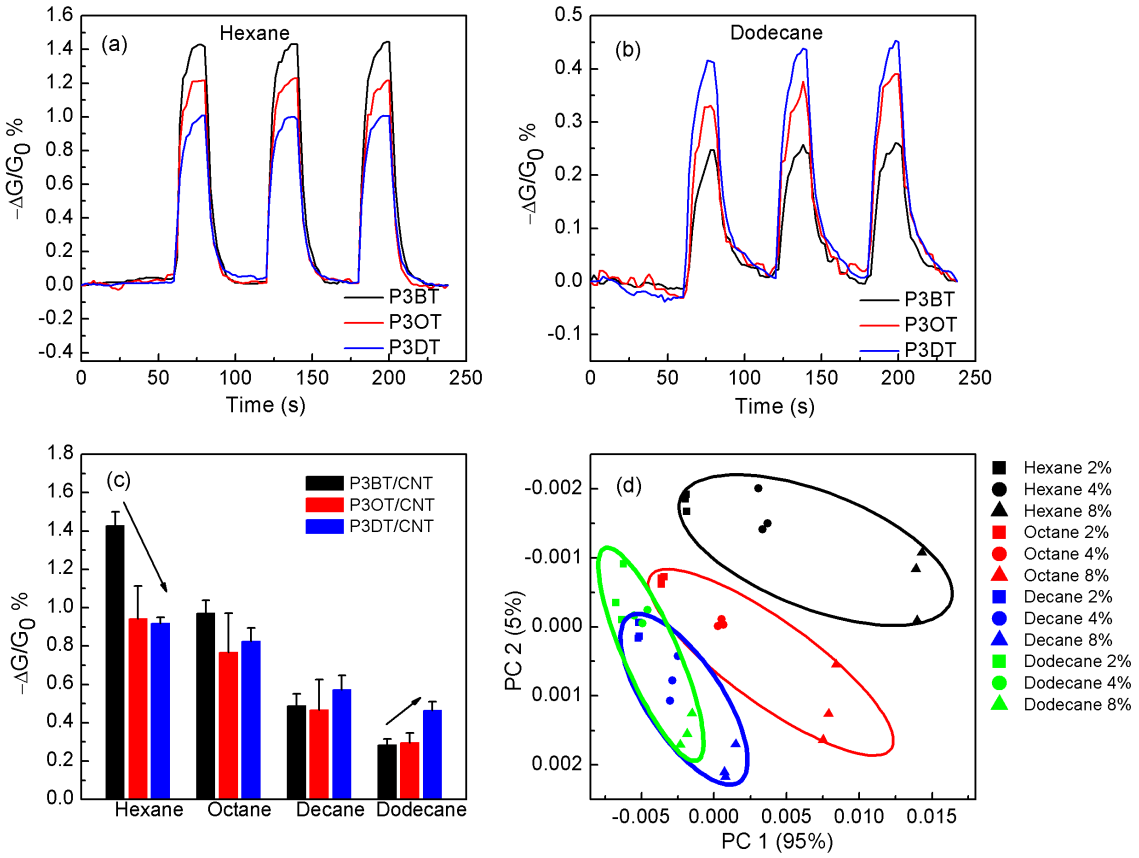

Figure 3.5 (a) Real-time sensors' responses to 8% of the saturated vapor of n-hexane from the P3BT/CNT sensor, the P3OT/CNT sensor and the P3DT/CNT sensor. (b) Real-time sensors' responses to 8% of the saturated vapor of n-dodecane from the same three sensors. (c) Summary of responses from the three kinds of sensors (three independent sensors for each type) to 8% of the saturated vapor of n-hexane, n-octane, n-decane, n-dodecane. (d) Principle component score plot of the sensor array containing the three P3AT/CNT sensors to four alkane analytes (three concentrations for each analytes, three trials each concentration).

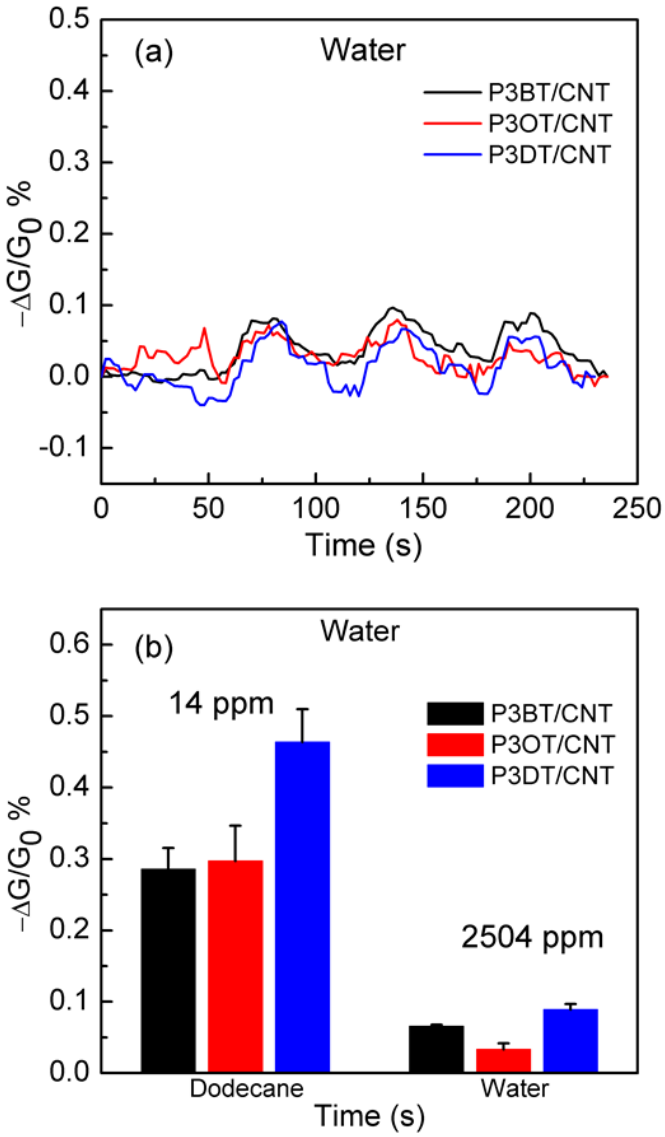

Figure 3.6 (a) Real-time sensor responses to 8% of water vapor. The analyte exposure time is 20 s and the recovery time is 40 s. (b) Comparison of the sensors' responses to n-dodecane and water.

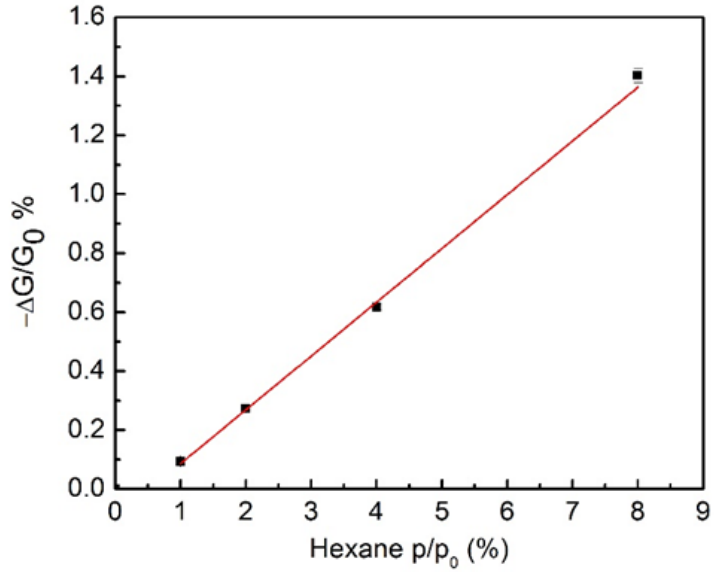

Figure 3.7 The linear fitting curve of the P3BT/CNT sensor's responses from 1%, 2%, 4%, and 8% of the saturated vapor of n-hexane. The analyte exposure time is 20 s and the recovery time is 40 s.

Table 3.1 Saturated vapor pressure of the four alkane analytes and water at 20 °C.

Analytes	P° (ppm)
n-hexane	173,600
n-octane	14,500
n-decane	1,920
n-dodecane	170
water	31,300

CHAPTER 4

SENSING METHAMPHETAMINE WITH CHEMIRESISTIVE SENSORS BASED ON POLYTHIOPHENE-BLENDED SINGLE-WALLED CARBON NANOTUBES[1]

4.1 Abstract

A highly sensitive and selective carbon nanotube-based vapor sensor was developed toward the detection of methamphetamine vapor, one of the most widespread, harmful and addictive illegal drugs in the world. Poly(3-(6-carboxyhexyl)thiophene-2,5-diyl)) (P3CT) was chosen to noncovalently functionalize carbon nanotubes, which can facilitate the suspension of carbon nanotubes in the solvents as well as introduce a carboxylic acid functional group. The carboxylic acid group in the polymer acts as a binder of organic amines via acid-base interaction. The P3CT-functionalized carbon nanotube sensors show sensitivity to n-methylphenethylamine (NMPEA), a detection simulant of methamphetamine, as low as 4 ppb. The sensors were able to distinguish NMPEA from two other amine compounds, various volatile chemical compounds (VOCs), and water vapor by observing the recoverability of the sensor's signal after exposure. The sensor

---

[1] Adapted with permission from Zhang, Y.; Bunes, R. B.; Wu, N.; Ansari, A.; Rajabali, S.; Zang, L., Sensing Methamphetamine with Chemiresistive Sensors Based on Polythiophene-Blended Single-Walled Carbon Nanotubes, Sens. Actuators B Chem. **2017**, http://dx.doi.org/10.1016/j.snb.2017.08.201. Copyright (2017) Elsvier.

showed higher sensitivity to amine vapors even when the vapor concentrations of amines were several orders of magnitude lower than those of the VOCs. Our research gives a simple but effective method for detecting trace amounts of methamphetamine in ambient air. Meanwhile, the sensor developed in this study can be used as one component in a next generation portable, intelligent, and low-cost chemical sensor array system for more complex real-life applications.

4.2 Introduction

N-methamphetamine (NMPA) is a highly addictive central nervous system stimulant and an illegal drug that is a worldwide health problem (1). The negative consequences of taking NMPA affect not only an individual's health but also his/her family and friends. The synthesis of NMPA is relatively simple and there are clandestine labs producing NMPA illegally worldwide (2). Meanwhile, these clandestine labs usually lack appropriate protection methods during the synthesis and often cause severe contamination of their local environment. Thus, a sensitive, portable, and reliable NMPA vapor sensor may be used to detect clandestine labs and drugs in transit.

Previous methods developed for detecting NMPA include gas chromatography (GC) (3), mass spectrometry (MS) (4), GC/MS (5), electrochemiluminescence (ECL) (6), Raman spectroscopy (7), liquid chromatography (8), surface ionization (9), and fluorescence sensors (10-13). Those sensing methods, especially those related to analytical instruments, have the advantage of accurate detection of trace amounts of NMPA in complex samples such as human urine and blood. They are used for screening for drug abuse. However, they have drawbacks of extensive sample preparation, expensive and cumbersome instruments, and complicated instrumental operation and not suitable for the applications of real-time

detection and monitoring of NMPA in law enforcement scenarios. Thus, a sensor for NMPA that is simple and affordable is still highly demanded.

Electronic sensors such as chemiresistive sensors (14-17) are promising to fulfill this demand, as they are usually simple and inexpensive to make (17). In a chemiresistive sensor, only source electrode and drain electrodes are needed for measurements of the signal and only small amount of the sensor materials (in the range of micro-grams) are needed for making a device. Chemiresistive sensors integrate with circuit boards easily and can be small in size; thus, a hidden detector that communicates wirelessly to a computer or a small cell phone accessory for NMPA detection is easy to achieve. Carbon nanotubes (CNTs) are promising materials to use because of their high property sensitivity to environmental changes (18), good conductivity, and availability for surface functionalization (19-21), Previous studies have shown numerous examples of CNT-based chemiresistive sensors for monitoring trace amounts of dangerous gases and chemical vapors such as carbon monoxide (22), hydrogen sulfide (23), and diethylchlorophosphate (24) in the environment. However, little to no work has been published on using carbon nanotubes as NMPA vapor sensors. Herein, we designed a chemiresistive sensor based on single-walled CNTs functionalized with a polythiophene derivative for the detection of trace NMPA vapor. Polythiophene has been demonstrated as an effective material to noncovalently functionalize CNTs and disperse them in solvents (25), We chose poly(3-(6-carboxyhexyl)thiophene-2,5-diyl)) (P3CT) (Figure 4.1a) because of the hypothesis that the carboxylic acid group in the polymer will facilitate the sensing of NMPA because the carboxylic acid tends to react with the amine group in the NMPA through acid-base interaction. We have demonstrated our hypothesis by directly comparing sensors functionalized with a very similar polymer without carboxylic acid functional group,

namely, poly(3-octylthiophene-2,5-diyl) (P3OT) (Figure 4.1a).

4.3 Results and Discussion

UV-vis absorption spectra (Figure 4.1d) were obtained from the P3CT/CNT suspension and the P3CT solution using an Agilent Cary 100 UV-Vis spectrophotometer. The UV-vis absorption spectra of P3OT/CNT suspension and P3OT solutions were reported in our previous study (26). The spectrum of the P3CT shows a broad absorption band with maximum absorption wavelength at around 515 nm and a weak shoulder peak around 600 nm, which is very similar to the previously reported UV-vis absorption spectra of poly(3-hexylthiophene) (27). Upon mixing with CNTs, the overall baseline of the absorption spectrum of P3CT/CNT is increased in comparison to the P3CT solution due to the absorption of CNTs in longer wavelength.

To test our sensors with NMPA, we used a simulant, n-methylphenethylamine (NMPEA), which has a chemical structure very similar with NMPA (Figure 4.1b). Figure 4.2a shows the response of a representative P3CT/CNT sensor to 4 ppb, 8 ppb, 16 ppb and 32 ppb of NMPEA vapor, which was 0.001%, 0.002%, 0.004% and 0.008% diluted from the saturated vapor of NMPEA (395 ppm under 25 °C) (28). The exposure to NMPEA vapor lasted 20 s and was followed by a recover period of 40 s. Each concentration of NMPEA was introduced to the sensor 3 times to test the reproducibility. Overall, the sensor's response to NMPEA is fast, large, and semi-recoverable (ranging from 10% to 50%). The sensor shows a clear response at concentrations as low as 4 ppb, indicating a limit of detection lower than 4 ppb for NMPEA. Figure 4.2b compares the responses of sensors comprised of P3CT/CNT, P3OT/CNT, and nonfunctionalized CNT sensor to different concentrations of NMPEA vapor tested simultaneously. The sensitivity of the

P3CT/CNT sensor towards NMPEA vapor is more than an order of magnitude greater than that of the nonfunctionalized CNT sensors and more than 6 times greater than that of the P3OT/CNT. This demonstrated the improved sensitivity of the P3CT/CNT sensor to NMPEA due to the carboxylic acid group of P3CT that enables strong binding with amines.

Selectivity of the P3CT/CNT sensor against other common chemicals is very important when the sensor is used in real-life applications. Thus, we tested the P3CT/CNT sensor to a number of common volatile organic compounds (VOCs) and water vapor at the concentration of 1% of their saturated vapor pressure, as well as, two amines (aniline and benzylamine) at the concentration of 0.008% of the saturated vapor. The selectivity of the P3CT/CNT sensor draws from two aspects. The first one is the recoverability of the response and the second is the sensitivity. Figure 4.3 shows the real-time response profiles of a P3CT/CNT sensor to aniline, benzylamine, toluene and ethyl acetate vapors. The sensor responds to the two amine vapors and after the exposure, the sensor seems to continue to respond but at a slower rate and does not recover. On the contrary, the sensor's responses to toluene and ethyl acetate vapor are fully recoverable (the same as observed for other vapors such as acetone, water and ethanol). This is interesting because we can simply distinguish amines and other common VOCs by observing the recovery behavior of the sensor. Moreover, the sensor also shows significantly higher sensitivity to amines than other VOCs. Figure 4.4 shows the responses of the three kinds of sensors to various VOCs at the concentration of 1% of their saturated vapor pressure (29) and also, 32 ppb of NMPEA vapor. Although the vapor concentration of NMPEA is more than four orders of magnitude lower than the VOCs, the P3CT/CNT sensor still shows about one order of magnitude higher response to NMPEA compared to its response to the VOCs. This dramatic difference in response sensitivity helps distinguish NMPEA from the common

VOCs.

The mechanism for the high sensitivity of the P3CT/CNT sensor to amines is probably a combination of the swelling effect of the conductive CNT network in a nonconductive polymer matrix and the intrinsic sensing response of bare CNTs to amines, considering the fact that there is always some surface area of CNT free from polymer coverage. The intrinsic response comes from the interfacial electron transfer from the electron-donating amines to the bare surface of CNT where is not covered by the polymer, which results in a decrease of the conductivity of the p-type CNTs. (18) Meanwhile, the swelling process also gives a decrease of conductivity when the sensor is exposed to the analytes (28). The carboxylic acid group in the P3CT acts as a receptor of amine compounds (24, 30-31) and could enhance the interaction between the amine compounds and the sensor materials.

The nonrecoverable response of the sensors after exposure to amine vapors may come from the intrinsic properties of the vapor itself, since they tend to be bound to the surface of CNT through charge transfer interaction. Additionally, the carboxylic acid in the P3CT may also decrease the recoverability of the sensor after exposure to amine compounds because of the acid-base reaction. The semi-recoverability of the P3CT/CNT sensor to NMPEA, which is different from the nonrecoverability of other amine compounds, may be due to the increased steric hindrance of NMPEA (a secondary amine), which may decrease the surface binding strength.

4.4 Conclusion

In conclusion, efficient sensors of NMPEA were developed by using CNTs functionalized with P3CT as the chemiresistive sensing materials. The sensors were made by simply drop-casting the P3CT/CNT suspension on the interdigitated electrodes (IDEs).

NMPEA was detected at concentrations as low as 4 ppb. The acid-base interaction between the amine compounds and the carboxylic acid groups in the polymer may be the reason of the extraordinary sensitivity of the P3CT/CNT sensor to amine compounds. The sensor was able to distinguish NMPEA from two other amines, various common VOCs. The selectivity of our sensor to NMPEA comes from both the recoverability of the sensor after exposure to the analytes and the much-enhanced sensitivity to amine compounds.

4.5 Experimental Methods and Materials

4.5.1 Materials

Regioregular P3CT and regioregular P3OT were purchased from Reike metals. Carbon nanotubes (SG65i, single walled, >95% semiconducting species) were purchased from SouthWest NanoTechnologies. All the other chemicals were purchased from Sigma Aldrich or Fisher and used as received. Amine compounds used in this study for the vapor testing were 99% or higher in their purity.

4.5.2 Device Fabrication Details

The method of making the P3CT/CNT in dimethyl sulfoxide (DMSO) and P3OT/CNT in 1,2-dichlorobenzene (*o*-DCB) is very similar to the method developed previously in our lab (26, 32). Briefly, CNTs were suspended in o-DCB (for P3CT/CNT suspension) or DMSO (for P3OT/CNT suspension) with a concentration of 1 mg/mL, followed by 2 h of sonication. P3CT was dissolved in *o*-DCB and P3OT was dissolved in DMSO with a concentration of 5 mg/mL. Then, the polymer solution and the CNT suspension in the corresponding solvent were mixed with a polymer:CNT weight ratio of 3:1. The mixtures were sonicated for 2 h and then diluted into corresponding solvents to achieve a

concentration of CNT of 2.5 μg/mL (estimated) and the diluted suspensions were sonicated again for 2 h. The final suspension of P3CT/CNT was purple to pink in color, and was darker than the solution with only P3CT in it. The suspension was stable without forming aggregates after 3 months while the CNT in DMSO formed aggregations after several days (see Figure 4.1c). Overall, the process of making CNT suspensions with P3CT and P3OT is simple, reproducible, and cost-effective.

The process of fabricating sensor devices is the same as we used in our previous study (26, 32). Sensors were fabricated by drop-casting the P3CT/CNT suspension or the P3OT/CNT suspension onto a pre-patterned interdigitated electrodes (IDEs) (the gap between fingers is 80 μm, see section in this dissertation for details of fabrication with standard photolithography process in a clean room). The IDE chip was then heated to 120 °C for 10 min in an ambient environment to remove the remaining solvent. After that, the electrical resistance of the IDE was tested. Drop-casting the suspension and drying was repeated until the resistance of the device reached 20 – 200 kΩ, forming a thin film of polymer/CNT on the IDEs.

4.5.3 Sensors Evaluation Details

The sensors were tested using a homemade chemical vapor generation and testing system. Saturated vapor of analytes other than amine-related analytes (including NMPA, aniline and benzylamine) were loaded into a glass syringe in a programmed syringe pump (NE-4000 New Era Pump System, Inc.). Amine related analytes were diluted 1000 times by volume before loading to the glass syringe. The analyte vapors in the syringe pump were pumped into a 100 sccm carrier gas (dry air) at rates of 1.01 sccm, 2.04 sccm, 4.17 sccm and 8.7 sccm to create analyte concentrations of 1%, 2%, 4%, and 8% of each

analyte's concentration in the glass syringe. The syringe pump was programed to infuse 20 s of the saturated analyte vapor into the carrier gas with a duty cycle of 60 s in order to achieve different diluted vapor concentrations of the analyte. The process was repeated three times to examine the reproducibility of sensor response. The diluted vapors were delivered to a PTFE chamber with sensors inside. The sensors were wire-bonded to a ceramic chip carrier and connected to an Agilent 4156C Precision Semiconductor Parameter Analyzer. The sensors were operated at a constant DC bias of 0.1 V and the electrical currents were monitored by the semiconductor analyzer. Matlab and Microsoft Excel were used to perform the baseline correction and the data analysis.

4.5.4 Definition of Recoverability

The recoverability is defended as:

$$\text{Recoverability} = (b-c)/(b-a)*100\% \quad (4.1)$$

where a, b, c are the sensor's normalized value as marked in a typical sensor response profile shown in Figure 4.5.

4.6 Acknowledgments

This work was supported by the Department of Homeland Security, Science and Technology Directorate under Grant (2009-ST-108-LR0005), the National Science Foundation under Grant #IIP-1059286 to the American Society for Engineering Education and USTAR program.

4.7 References

(1) http://www.drugfreeworld.org/drugfacts/crystalmeth.html. What ismethamphetamine?

(2) National Drug Threat Assessment, National Drug Threat Assessment, NationalDrug Intelligence Center; U. S. Department of Justice, Johnstown, PA, 2006.

(3) H. Inoue, K. Kuwayama, Y.T. Iwata, T. Kanamori, K. Tsujikawa, H. Miyaguchi,Simple and simultaneous detection of methamphetamine and dimethylsulfone in crystalline methamphetamine seizures by fast gaschromatography, Forensic Toxicol. 26 (2008) 19–22.

(4) R.D. Espy, S.F. Teunissen, N.E. Manicke, Y. Ren, Z. Ouyang, A. van Asten, R.G.Cooks, Paper spray and extraction spray mass spectrometry for the direct and simultaneous quantification of eight drugs of abuse in whole blood, Anal. Chem. 86 (2014) 7712–7718.

(5) P. Basilicata, M. Pieri, V. Settembre, A. Galdiero, E. Della Casa, A. Acampora, N. Miraglia, Screening of several drugs of abuse in italian workplace drug testing: performance comparisons of on-site screening tests and a fluorescence polarization immunoassay-based device, Anal. Chem. 83 (2011) 8566–8574.

(6) H. Dai, Y. Wang, X. Wu, L. Zhang, G. Chen, An electrochemiluminescent sensorfor methamphetamine hydrochloride based on multiwall carbonnanotube/ionic liquid composite electrode, Biosens. Bioelectron. 24 (2009)1230–1234.

(7) P. Vandenabeele, H.G.M. Edwards, J. Jehlicka, The role of mobileinstrumentation in novel applications of Raman spectroscopy: archaeometry, geosciences, and forensics, Chem. Soc. Rev. 43 (2014) 2628–2649.

(8) M. Concheiro, A. de Castro, O. Quintela, M. López-Rivadulla, A. Cruz,Determination of MDMA, MDA, MDEA and MBDB in oral fluid using highperformance liquid chromatography with native fluorescence detection, Forensic. Sci. Int. 150 (2005) 221–226.

(9) A. Hackner, S. Beer, G. Müller, T. Fischer, S. Mathur, Surface ionization detection of amphetamine-type illicit drugs, Sens. Actuators B Chem. 162(2012) 209–215.

(10) M. He, H. Peng, G. Wang, X. Chang, R. Miao, W. Wang, Y. Fang, Fabrication of anew fluorescent film and its superior sensing performance toN-methamphetamine in vapor phase, Sens Actuators B Chem. 227 (2016)255–262.

(11) D. Wen, Y.Y. Fu, L.Q. Shi, C. He, L. Dong, D.F. Zhu, Q.G. He, H.M. Cao, J.G. Cheng, Fine structural tuning of fluorescent copolymer sensors formethamphetamine vapor detection, Sens. Actuators B Chem. 168 (2012)283–288.

(12) Y. Che, L. Zang, Enhanced fluorescence sensing of amine vapor based onultrathin nanofibers, Chem. Commun. 34 (2009) 5106–5108.

(13) Y. Che, X. Yang, S. Loser, L. Zang, Expedient vapor probing of organic aminesusing fluorescent nanofibers fabricated from an n-type organicsemiconductor, Nano Lett. 8 (2008) 2219–2223.

(14) N. Wu, C. Wang, B.R. Bunes, Y. Zhang, P.M. Slattum, X. Yang, L. Zang, Chemical self-doping of organic nanoribbons for high conductivity and potential application as chemiresistive sensor, ACS Appl. Mater. Interfaces 8 (2016)12360–12368.

(15) C. Wang, N. Wu, D.L. Jacobs, M. Xu, X. Yang, L. Zang, Discrimination of alkyland aromatic amine vapors using TTF-TCNQ based chemiresistive sensors, Chem. Commun. 53 (2017) 1132–1135.

(16) H. Huang, D.E. Gross, X. Yang, J.S. Moore, L. Zang, One-Step surface doping oforganic nanofibers to achieve high dark conductivity and chemiresistor sensing of amines, ACS Appl. Mater. Interfaces 5 (2013) 7704–7708.

(17) S.F. Liu, A.R. Petty, G.T. Sazama, T.M. Swager, Single-walled carbon nanotube/metalloporphyrin composites for the chemiresistive detection ofamines and meat spoilage, Angew. Chem. Int. Edit. 54 (2015) 6554–6557.

(18) J. Kong, N.R. Franklin, C. Zhou, M.G. Chapline, S. Peng, K. Cho, H. Dai, Nanotubemolecular wires as chemical sensors, Science 287 (2000) 622–625.

(19) B.R. Bunes, M. Xu, Y. Zhang, D.E. Gross, A. Saha, D.L. Jacobs, X. Yang, J.S. Moore,L. Zang, Photodoping and enhanced visible light absorption in single-walled carbon nanotubes functionalized with a wide band gap oligomer, Adv. Mater.27 (2015) 162–167.

(20) H. Peng, L.B. Alemany, J.L. Margrave, V.N. Khabashesku, Sidewall carboxylicacid functionalization of single-walled carbon nanotubes, J. Am. Chem. Soc.125 (2003) 15174–15182.

(21) M. Ding, Y. Tang, P. Gou, M.J. Reber, A. Star, Chemical sensing with polyaniline coated single-Walled carbon nanotubes, Adv. Mater. 23 (2011) 536–540.

(22) S.F. Liu, S. Lin, T.M. Swager, An Organocobalt–Carbon nanotube chemiresistive carbon monoxide detector, ACS Sensors 1 (2016) 354–357.

(23) H.Y. Jung, Y.L. Kim, S. Park, A. Datar, H.-J. Lee, J. Huang, S. Somu, A. Busnaina,Y.J. Jung, Y.-K. Kwon, High-performance H2S detection by redox reactions in semiconducting carbon nanotube-based devices, Analyst 138 (2013)7206–7211.

(24) A.W. Snow, M.G. Ancona, Sensitivity, selectivity, and nanodimensional effectsin gold nanocluster vapor sensors, IEEE Sens. J. 14 (2014) 3330–3336.

(25) H. Gu, T.M. Swager, Fabrication of free-standing, conductive, and transparentcarbon nanotube films, Adv. Mater. 20 (2008) 4433–4437.

(26) Y. Zhang, B.R. Bunes, C. Wang, N. Wu, L. Zang,Poly(3-alkylthiophene)/CNT-based

chemiresistive sensors for vapor detectionof linear alkanes: effect of polymer side chain length, Sens. Actuators B Chem.247 (2017) 713–717.

(27) T.-A. Chen, X. Wu, R.D. Rieke, Regiocontrolled synthesis ofpoly(3-alkylthiophenes) mediated by rieke zinc: their characterization and solid-State properties, J. Am. Chem. Soc. 117 (1995) 233–244.

(28) Royal Society of Chemistry ChemSpider. N-Methylphenethylamine, PredictedACD/Labs; http://www.chemspider.com/Chemical-Structure.11019.html?rid = 25053312-642a-4683-a454-b62dd4c71e41 (Accessed Junly 27, 2017).

(29) J.M. Schnorr, D. van der Zwaag, J.J. Walish, Y. Weizmann, T.M. Swager, Sensoryarrays of covalently functionalized single-walled carbon nanotubes forexplosive detection, Adv. Funct. Mater. 23 (2013) 5285–5291.

(30) Y. Zhang, M. Xu, B.R. Bunes, N. Wu, D.E. Gross, J.S. Moore, L. Zang,Oligomer-coated carbon nanotube chemiresistive sensors for selective detection of nitroaromatic explosives, ACS Appl. Mater. Interfaces 7 (2015)7471–7475.

(31) T. Gao, E.S. Tillman, N.S. Lewis, Detection and classification of volatile organicamines and carboxylic acids using arrays of carbon black-dendrimercomposite vapor detectors, Chem. Mater. 17 (2005) 2904–2911.

(32) T. Wang, S. Korposh, S. James, R. Tatam, S.W. Lee, In Polyelectrolyte MultilayerNanothin Film Coated Long Period Grating Fiber Optic Sensors for AmmoniaGas Sensing, 13th IEEE International Conference on Nanotechnology, 2013,pp. 505–508.

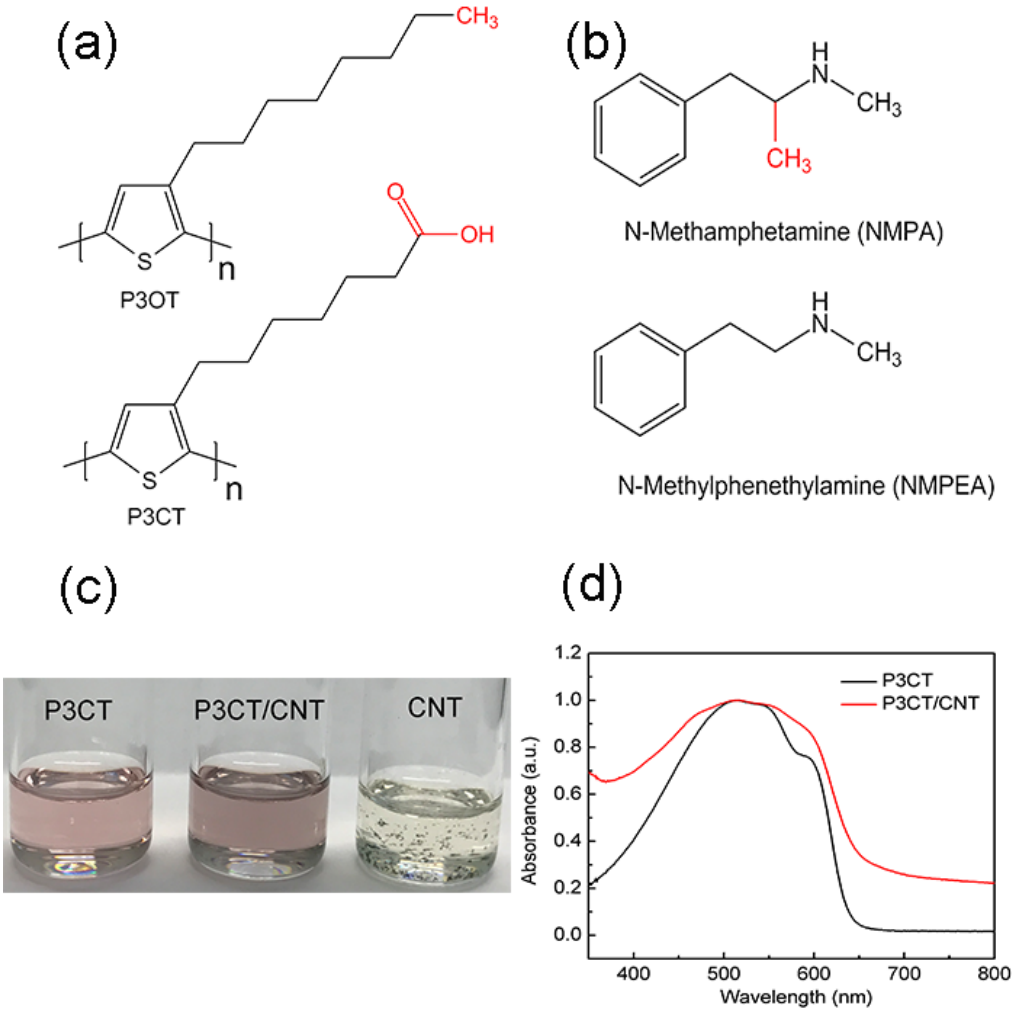

Figure 4.1 (a) Molecular structures of two polythiophene derivatives (P3OT and P3CT) for noncovalent functionalization of CNTs. (b) Molecular structure of NMPA and its analog NMPEA which was used in the vapor sensing tests. (c) Photos of P3CT (7.5 μg/mL), P3CT/CNT and CNT in DMSO. (d) UV-vis spectra of P3CT and P3CT/CNT in DMSO.

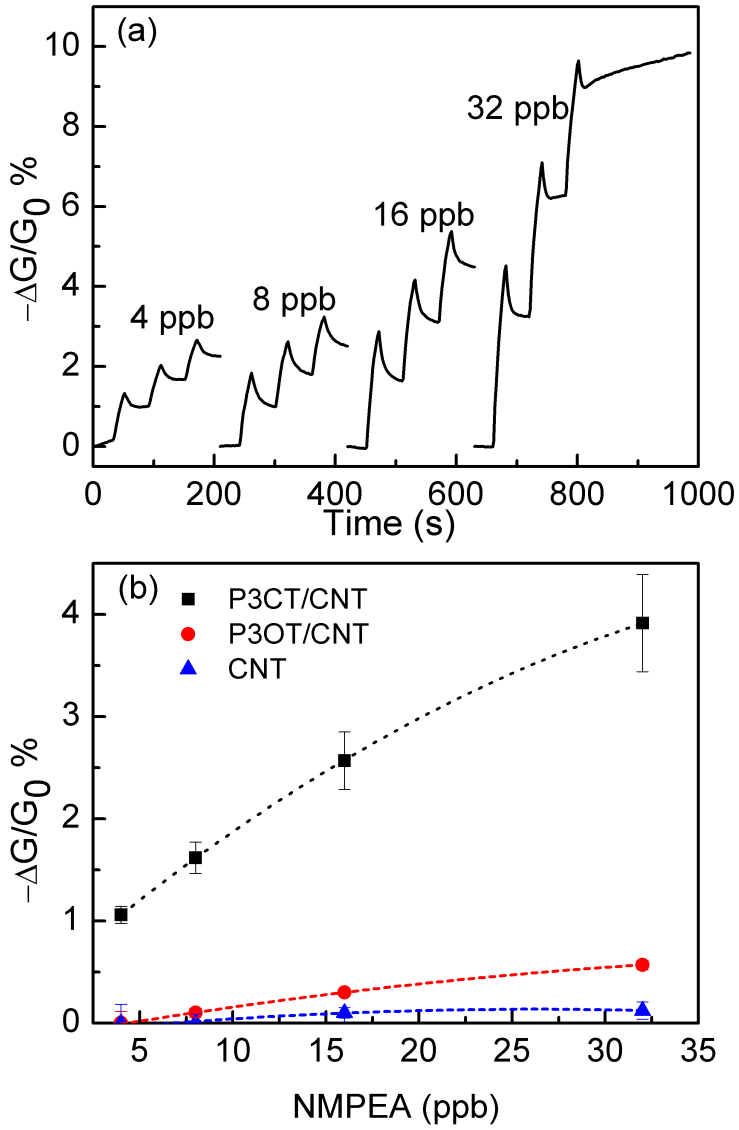

Figure 4.2 (a) Real-time sensing responses of a P3CT/CNT sensor towards 4 ppb, 8 ppb, 16 ppb and 32 ppb of NMPEA vapor. The vapor exposure time is 20 s followed by a 40 s recovery time. (b) Responses of a P3CT/CNT sensor, a P3OT/CNT sensor, and a non-functionalized CNT sensor to different concentrations of NMPEA vapor in the same testing environment (dashed lines are the quadratic fitting).

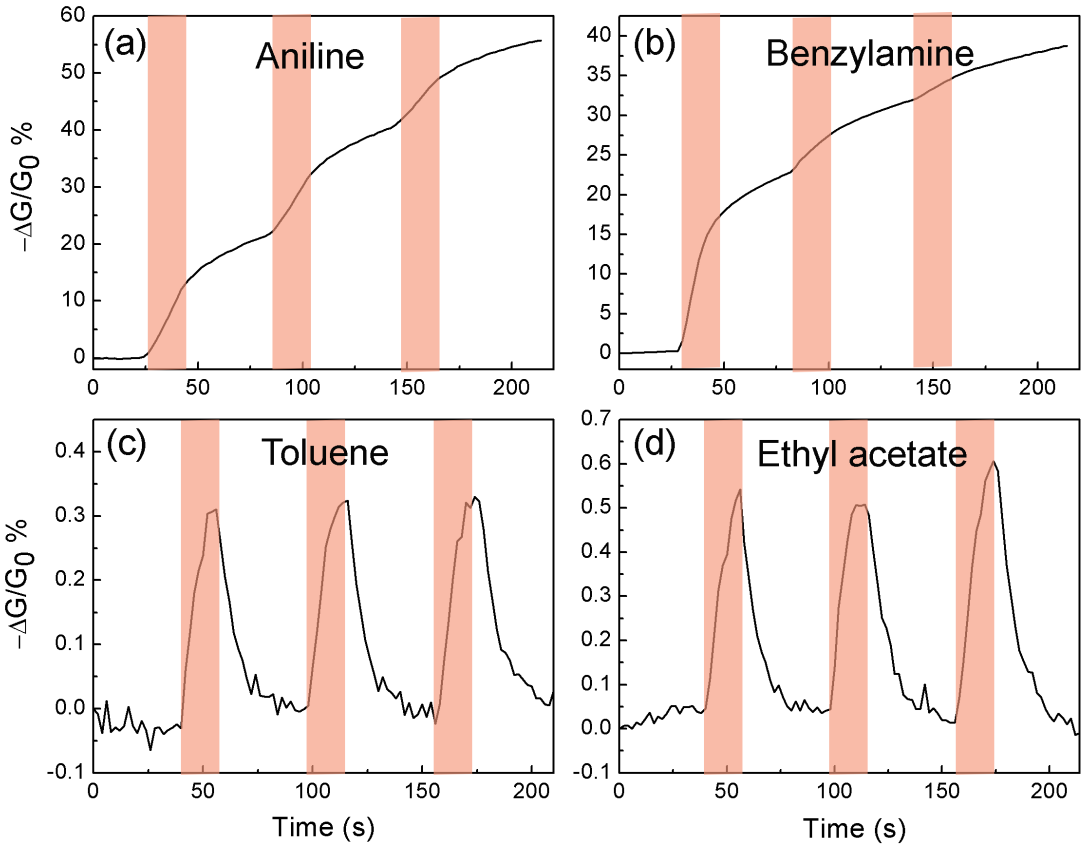

Figure 4.3 Real-time sensor's responses to vapors of aniline (64 ppb), benzylamine (74 ppb), toluene (375 ppm), and ethyl acetate (1244 ppm) from a P3CT/CNT sensor. The colored bars represent the time when analyte vapors expose to the sensor.

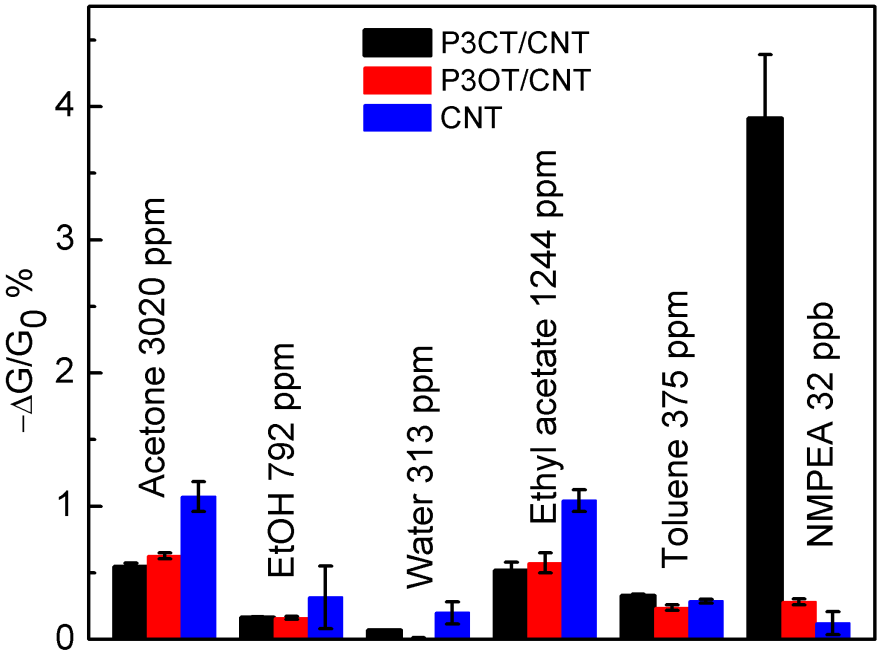

Figure 4.4 Responses of the P3CT/CNT sensor, the P3OT/CNT sensor, and the non-functionalized CNT sensor to 20 s vapor exposures of various compounds (1% of saturated vapor) and 32 ppb of NMPEA. Note: the vapor concentration of NMPEA is more than four orders of magnitude lower than the reference VOCs.

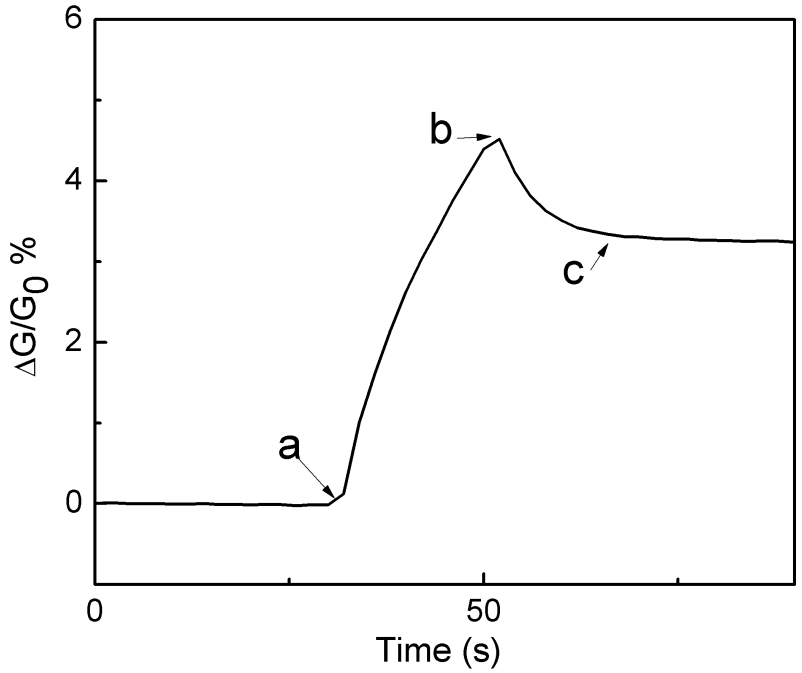

Figure 4.5 Real-time sensor response to NMPEA vapor. Arrow-a points to the beginning of the vapor exposure. Arrow b marks when the vapor exposure ends. Arrow c points the estimated time when the sensor recovers and reaches a plateau.

CHAPTER 5

DISSERTATION CONCLUSIONS AND PROPOSED FUTURE WORK

5.1 Dissertation Conclusions

A low-cost, portable, and reliable vapor sensing method is extremely desired for the application of explosive and drug detection. CNT-based chemiresistive sensors have shown great promise to this application, while technical challenges still exist. One of the biggest challenges is the lack of selectivity in order to be used in the complex real-life situations. In this dissertation, several functionalization materials for enhancing the sensors' selectivity were explored and studied. Chapters 2 to 4 in this dissertation describe different types of sensors and the differential sensing based on them. The sensors can be used for the selective detection of nitro-explosives (TNT, DNT, and NT), improvised explosive made of ammonium nitrate-fuel oil (alkanes), and methamphetamine.

In Chapter 2, the CNT sensors functionalize with oligomers were able to distinguish TNT vapors from common VOCs, such as acetone, water, and ethanol. The oligomer used in this study can facilitate the dispersion of CNTs and enhance the absorption of TNT on the surface of them. The dominant mechanism of the sensors is due to the swelling of the oligomer on the surface of the CNT network.

In Chapter 3, the sensors were able to distinguish four different linear alkanes based on

their lengths. The polymers we used for functionalize CNTs were P3ATs with three different side-chain lengths. It was shown that the sensors coated with P3HTs with longer side-chain lengths will react most to alkane vapors similar to the side-chain lengths. By comparing the responses from different P3AT/CNT sensors, we can distinguish the lengths of the linear alkanes.

In Chapter 4, the sensors made from CNTs coated with P3CT were able to distinguish amine vapors from common VOCs. The sensor's ability to distinguish amines comes from both the carboxylic functional group in the polymer and the different kinetics of the sensor's recovery after exposing to different analytes. Thus, the amplitude of sensors' response and the sensors' recovery pattern can be used for the selective detection of amine-related drugs.

5.2 Suggestions for Future Work

5.2.1 For Fundamental Research

The following suggestions are recommended for future fundamental researches on the vapor detection of explosives and drugs based on CNT sensors:

1. We have proposed a sensing mechanism which is due to the swelling of the interfacial oligomer wrapped on CNTs. Nanoscale morphology changes observed from high-resolution AFM will be useful to demonstrate this mechanism directly.
2. A chemometric model that correlates the concentrations of the analytes with the responses of the sensors will be helpful for us to further optimize the fabrication parameters. Those fabrication parameters include the polymer/CNT ratio, the thickness of the thin film, and the type of CNTs used in the study. Note: the CNTs used in our study are a mixture of several kinds of CNTs with different chiralities.

3. Future work on the alkane sensors can rely on changing the polymer's side chain length or side chain structure from linear to branched, so that we can target on broader sizes of alkanes. Alternatively, we may work on changing the side chains of the polymer from saturated hydrocarbon ones to unsaturated ones, so that we can target on unsaturated hydrocarbon analytes like alkenes.
4. In Chapter 4, we demonstrated the feasibility to change the functional group of the polymer side chain to enable a specific binding to certain analytes (e.g., carboxylic group towards amines). Future work along this line can be centered on changing the functional group of the side chains from current single carboxylic group to multiple carboxylic groups to target on more complicated amines like some drugs. Furthermore, we can also change the functional group to be carbazole-related chemicals to target on nitroaromatic explosives like TNT.

5.2.2 For Practical Usage and Commercialization

The following suggestions are recommended for practical usage and commercialization on the vapor detection of explosives and drugs based on CNT sensors and beyond:

1. By improving the fabrication methods for the CNT thin film, we can increase the yield of device fabrication and enhance the sensitivity of the sensors. We can further optimize the parameters of the current fabrication method, and consider other fabricaton methods, such as spray-coating, spin-coating, doctor-blade, ink-printing and so on.
2. Researchers can develop sensors with different substrates, such as plastics, papers, and textiles, aiming at wearable sensors, disposable sensors, and sensor stickers.
3. Researchers can integrate the sensors with wireless communication systems,

particularly those controlled by a smart phone. This will definitely make the CNT sensors easier to use and secure access to customers.

4. The appropriate storage methods need to be studied as well to ensure the stable sensor performance and the extended lifetime of the sensors, which is a common issue for almost all the electrical sensors since a lot of environmental facts (such as humidity, temperature, and oxygen in the air, etc.) may affect the sensors' performance. This is extremely important for the noncovalently functionalized CNT sensors, since the performance of those devices degrade with time relatively faster than the covalently functionalized CNT sensors.
5. The calibration methods will be useful for minimizing device-to-device differences. The calibration will be required just after the fabrication of sensor devices, and required before the use and before the re-use of the devices.
6. The standards for validating sensor devices' performance and properties are highly desired. Since different research labs are testing their sensors using different methods (e.g., different flow rates and different exposure times), it's difficult to compare sensors between different research labs. Thus, a standard protocol for sensor testing and a shared database of the testing results will provide people with a better understanding of the sensors' performance comparing with other similar counterparts.